Structure Elucidation of Macrocyclic complex

1. Elemental analysis

The stoichiometries and chemical composition of the complexes proposed were supported by chemical analysis and conductance data (Table.1). All complexes are stable in air and non-hygroscopic. They are soluble in highly polar organic solvents such as DMF and DMSO, partially soluble in water and non-polar solvents. The metal ion concentrations were determined by using atomic absorption spectra and EDTA titration, while the number of coordinated water molecule attached per metal complex was determined by the dehydration method. Carbon, hydrogen and nitrogen (C,H,N) analysis was also done. The results of analysis along with the proposed chemical formula of the prepared complexes are given in Table (1).

2. Molar conductivities of metal complexes

Conductivity measurements in non-aqueous solutions have frequently been used in structural studies of metal chelates within the limit of their solubilities. They provide a method of testing the degree of ionization of the complexes. The more ions that a complex liberates in solution, the higher will be its molar conductivity and the non-electric complexes have negligible values of conductance. The molar conductivities of the prepared metal complexes were measured in solution of DMF. The molar conductance Λ_m (ohm^{-1} cm^{-2} mol^{-1}) is given by the relation:

$$\Lambda_m = K/C$$

Where Λ_m is molar conductance (omh^{-1} cm^2 $mole^{-1}$),K is the specific conductivity (ohm^{-1}) and C is the chelat concentration (mole/1).

The molar conductance values of the prepared complexes (Table 1) show a variation from non-electrolytic to electrolytic values according to the nature of ligand molecules. The data showed that the majority of the prepared complexes are of electrolytic nature and the cationic chelates are electrically balanced by the anion (chloride anion) outside the coordination sphere.

Elemental analysis and molar conductivity measurements showed the presence of Cl^- ion outside coordination sphere. During thermal degradation of such complexes, the removal of Cl^- ion in the form of HCl is expected to take place at 270-350 °C[59]. In the case of Ni(o-phenylenediamine-acetylacetone) complex, the weak exothermic peak at 380 °C is due to the removal of HCl, but no obvious weight loss appears correspondingly at the TG curve, perhaps due to the very vast thermal degradation of this complex.

3. Thermogravimetric and Differential Thermal Analysis of some Macro Complexes

Thermal methods of analysis introduce a new possibility for the investigation of metal chelates. They include such techniques as thermogravimetric analysis (TGA), differential thermal analysis (DTA) and thermometric titration (TT). In the present study only the first two methods are utilized. From TGA curves, one can calculate the percentage of hygroscopic and coordinated water molecules as well as metal ions in chelate. On the other hand, these of DTA make it possible to characterize, thermodynamically, the process of phase transformation in the examined system[60]. To understand the mechanism of complex formation and stability of the complexes so formed, it is of interest to observe the intermediate products formed by oxidative action of heat on the investigated metal chelates.

The present investigation is a study of the thermogravical behavior of some selected Ni^{+2}, Co^{2+} and Cu^{2+} complexes as a representative examples of the newly prepared macro complexes. Fig. (2) shows the TG and DT curves of nickel(II) complexes prepared by template reaction of $NiCl_2$ with o-phenylenediamine and acetylacetone. The curves shows that each endo-or exothermic peak on the DT curve corresponding to certain phase transformation and is accompanied by an inflection on the TG curve from which the corresponding weight loss can be calculated. The DT curve of the investigated Ni^{2+}complex show an exothermic peak at 125°C with percent weight loss of 7% which is due to the removal of coordinated water molecule. The thermal decomposition of the CH_3 and CH_2 groups at temperature range from 140°C up to 530°C support the proposed structure. The CH_3 groups start to decompose at 140°C followed by CH_2 groups and the condensations of nitrogen atoms to give N_2 gas. The theoretical calculations of the percent of the CH_3, CH_2 and N groups to the total

molecular weight of the prepared compound are in agreement with the percent weight loss observed from the TG curve. The percentages of physical and coordinated water molecules are calculated from the inflection on the TGA curve accompanying these peaks and are given in Table (2).

The unhydrated Ni^{2+} complex shows thermal stability up to 300 °C at which it starts single step decomposition till 530 °C. This is shown by the series of exothermic peaks at 350-500 °C indicating the decomposition of the complex leading to the formation of NiO_2 as final oxidative product. This is identified quantitatively from the steady state, TG curve after decomposition process.

From these results we can suggest a thermal degradation pattern of this complex as follow:

$$[Ni\ (L)(H_2O)_x]\ Cl_x \xrightarrow{125\ ^\circ C\ (7\%)} [Ni\ (L)]\ Cl_x + x\ H_2O$$

$$[Ni\ (L)]\ Cl_x \xrightarrow{380\ ^\circ C} [Ni\ (L)] + HCl\uparrow$$

$$[Ni\ (L)] \xrightarrow{530\ ^\circ C} NiO$$

Figures (3) and (4) represent the themograms (TG and DT curves) of Co^{2+}-o-phenylenediamine-acetylacetone and Co^{2+}-o-phenylene-benzoyl acetone, respectively. Inspection of Fig. (3) indicates that the macrocyclic complex of Co^{2+} with o-phenylenediamine-acetylacetone degrades through four steps represented by the exothermal peaks at 70, 125, 240 and 390 °C. Each of the peaks is accompanied by an inflection on the TG curve representing certain weight loss due to thermal fragmentation of the complex. Peak assignment and corresponding weight loss are given in Table (2). The first decomposition step at 70 °C is due to dehydration of adsorbed water molecule, the second at 125 °C is due to decomposition of CH_3 and CH_2 groups, the third at 240 °C is due to removal of Cl^- ion as HCl

while the final step started at 390 °C is due to the decomposition of the unhydrous complex leading to CoO as final product.

The thermal decomposition of Co^{2+} - o-phenylenediamine and benzoyl acetone complex takes place via three main steps. The first step in the decomposition sequence is a composite one being represented by one weight loss stage accompanied by two exothermic peaks at 70 and 80°C. This step is due to removal of both physically and coordinated water molecules. The second step represented by the strong exothermic peak at 275 °C is due to decomposition of complex matrix leading to $Co(NO_3)$ which decompose in the final step at 675 °C giving rise to CoO as a final decomposition product.

Figure (5) represents the DT and TG curves of Cu(o-phenylene-diamine and acetylacetone) complex which degrade in three steps. The removal of coordinated water molecules from the crystal lattice is represented by the exothermic peak started at 85 °C accompanied by 10% weight loss. The decomposition of the unhydrous complex started at 285 °C to 470 °C with weight loss 59 % due to evolution of CO_2 and H_2O vapour from the organic part of the complex. The last step started at 570 °C is due to the decomposition of Cu (NO_3) into CuO as final product. Table (2) lists peak positions, corresponding temperature and assignment of fragmentation products of the investigated complex.

From the thermal analysis of these complexes it is found that thermal stability of the investigated complexes lies in the order:
Co(o-phenylenediamine-acetylacetone) > Co(o-phenylenediamine- benzoyl acetone) > Cu(o-phenylenediamine-acetylacetone) > Ni(o-phenylene-diamine-acetylacetone).

Table (2): Termogravimetric analysis of the investigated Ni^{2+},Co^{2+} and Cu^{2+} complexes.

Complex	Temp.(°C)	Weight loss %	Assignment
Ni(o-phenamine-acac)	100-180 °C	7%	2.5 H_2O
	300-350 °C	34%	CO_2 +N_2 + H_2O
	>530 °C	59%	NiO_2 (residue)
Co(o-phenamine-acac)	70-125 °C	5%	1.5 H_2O
	200-230 °C	4%	Cl_2
	230-570 °C	64%	N_2+ CO_2+ H_2O
	>570 °C	27%	CoO(residue)
Co(o-phenamine-benzac)	70-170 °C	12%	4.5 H_2O
	275-400 °C	28%	CO_2 + H_2O
	675-740 °C	12%	NO_2
	>740 °C	48%	CoO (residue)
Cu(o-phenamine-acac)	85 °C	10%	3 H_2O
	285-470 °C	59%	CO_2+ H_2O
	570-590 °C	4%	NO_2
	>590 °C	27%	CuO(residue)

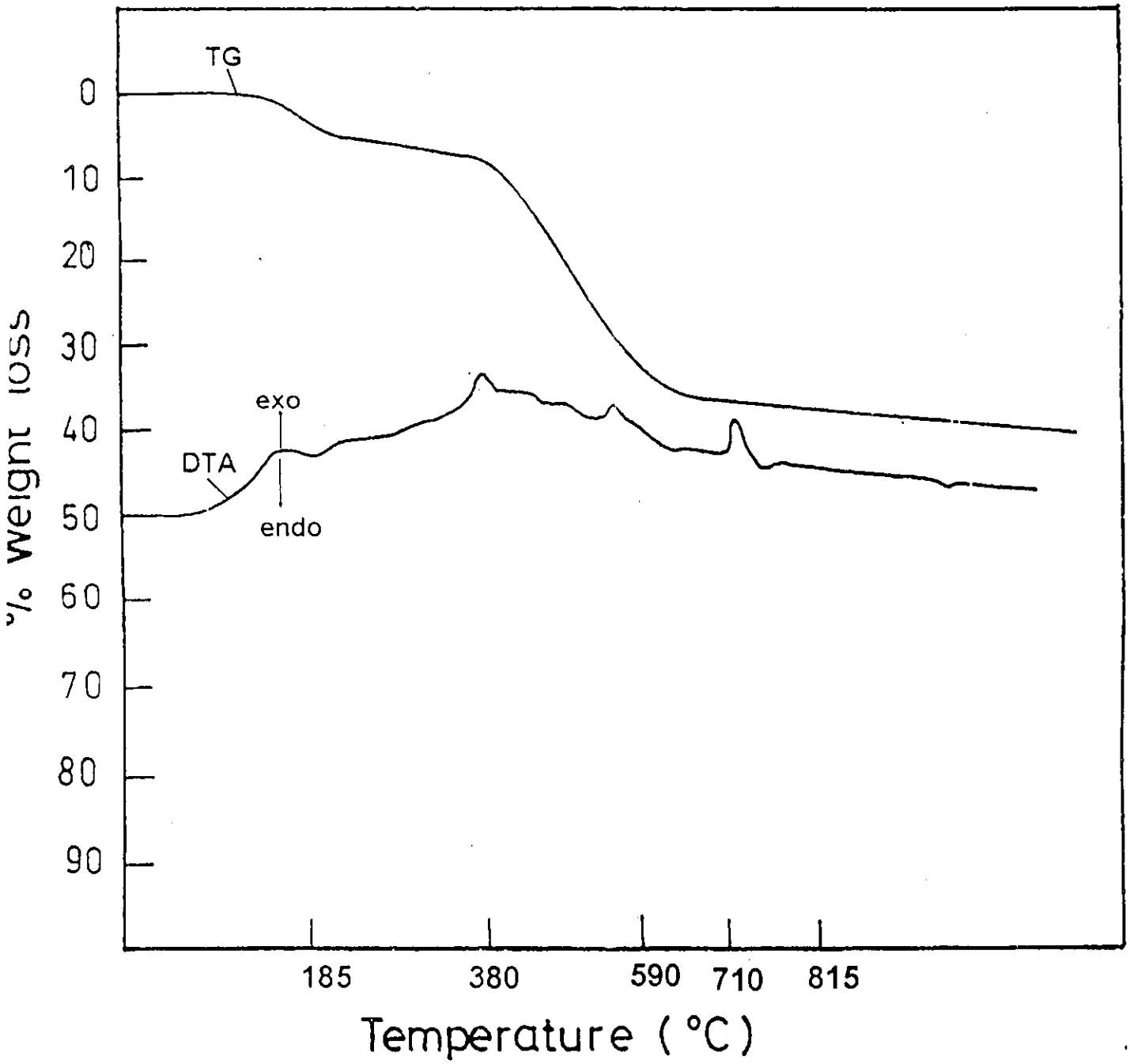

Fig. (2): Thermogravimetric and differential thermal curves of Ni^{2+}- o-phenelendiamine acetylacetone complex.

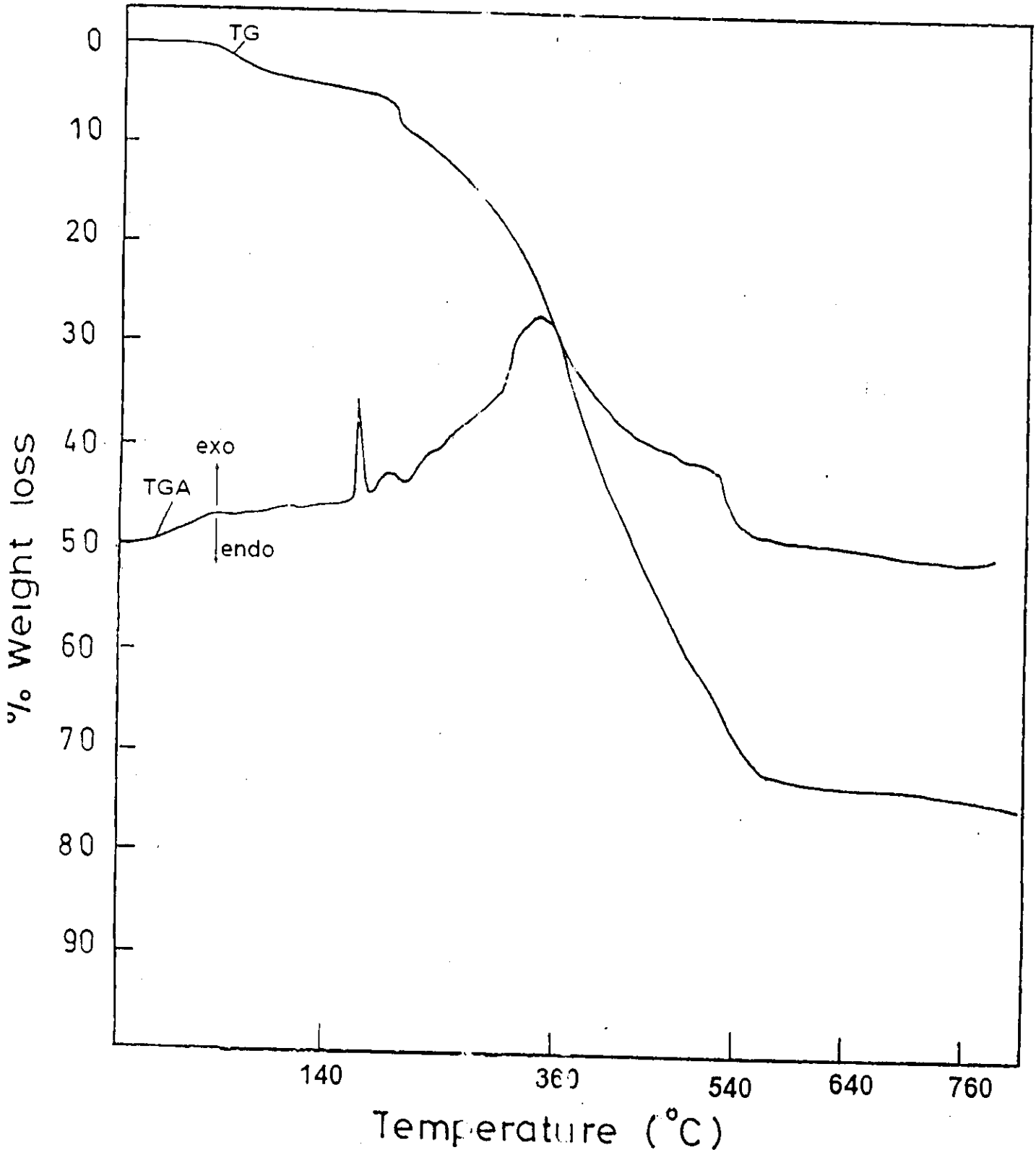

Fig. (3): Thermogravimetric and differential thermal curves of Co^{2+}-o-phenelendiamine-acetylacetone complex.

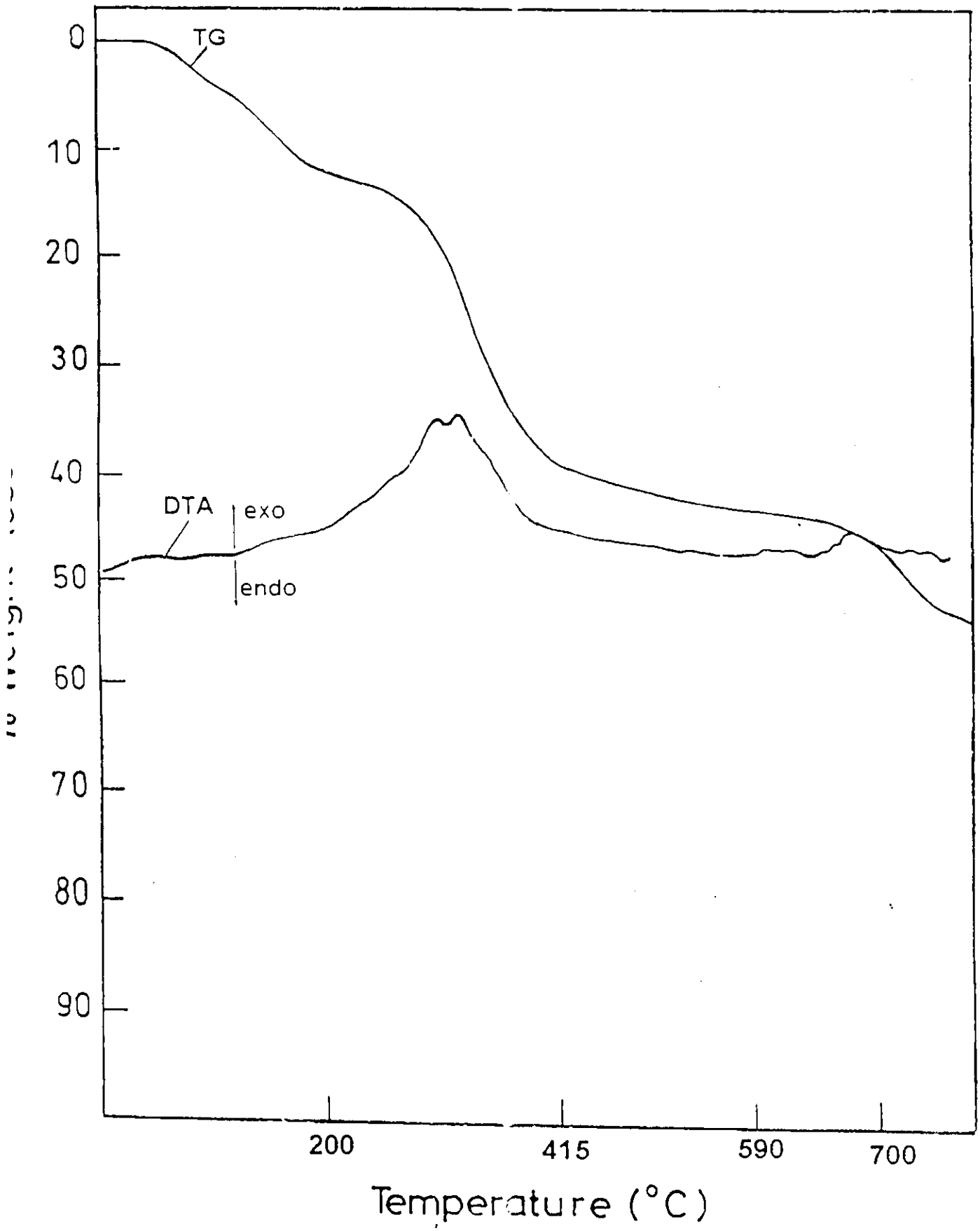

Fig. (4): Thermogravimetric and differential thermal curves of Co^{2+}-o-phenelendiamine-benzoylacetone complex.

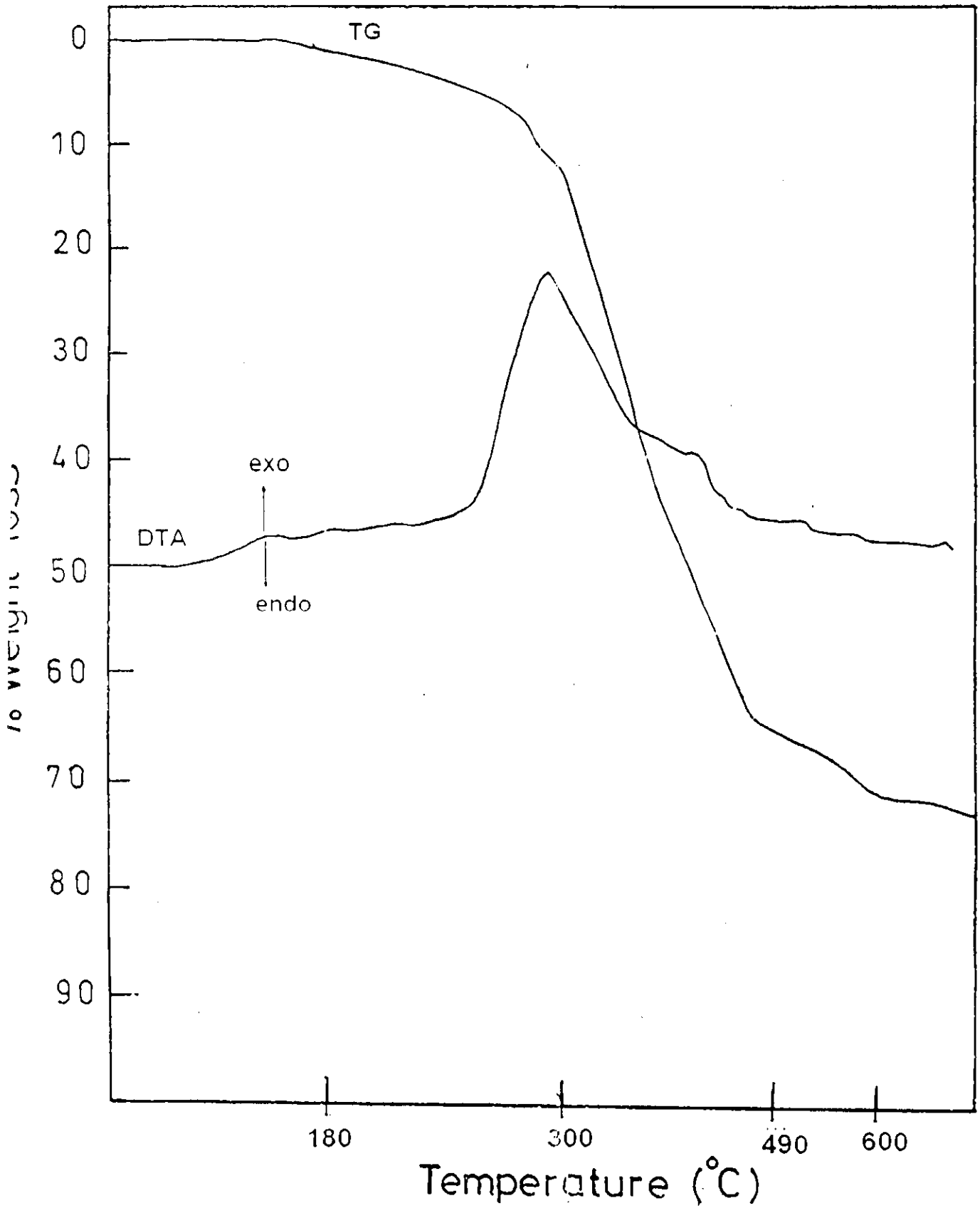

Fig. (5): Thermogravimetric and differential thermal curves of Cu^{2+}-o-phenelendiamine acetylacetone complex.

4. Infrared Spectra of Macrocyclic Complexes

A substantial part of the knowledge concerning the structure confirmation and mode of bonding in metal chelates can be gained by applying infrared spectroscopy either in absorbance or reflectance arrangements [61-63]. An insight in the type of bonds formed between the ligand and central metal ion can be achieved by careful investigation of the spectrum of complex compound essentially in comparison to that of the free ligand.

4.i. IR spectra of macrocyclic complexes formed between o-phenylenediamine and acetylacetone, benzoylacetone and dibenzoylmethane:

The IR-spectra of Fe^{3+}, Co^{2+}, Ni^{2+} and Cu^{2+} macrocyclic complexes with o-phenylenediamine and acetylacetone are studied and compared to those of the free organic compounds. The spectra are represented in Figs. (6-8) and the data are listed in Table (3).

An examination of the IR spectra showed that some ligand bands are completely disappeared or shifted due to lattice effect or due to departure from idealized symmetry [64]. The IR spectrum of o-phenylenediamine shows broad bands at 3362 cm^{-1} which is due to the stretching vibrational mode of the NH_2 groups. The strong band at 1630 $cm^{-1}$is due to the stretching vibration of the C=C in aromatic ring. The IR spectra of Fe^{3+}, Co^{2+}, Ni^{2+} and Cu^{2+} complexes do not show the first two bands with the appearance of new sets of bands at 1602-1659 cm^{-1}due to the stretching vibration of the C=N group ($\upsilon_{sym.C=N}$) resulting from the condensation of C=O and NH_2 groups of the acetylacetone and o-phenylenediamine respectively in the template reaction. Also, the asymmetric stretching vibration ($\upsilon_{asym.C=N}$) of this group gives new bands within the range 1114-1226 cm^{-1}. These bands are found at so lower frequencies probably due to

the participation of the nitrogen atom of the azomethine group in the coordination bonds [65]. This is supported by the disappearance of the strong band at 1655 cm^{-1} due to the stretching vibration of the C=O expected to present in the diketone molecule. In all complexes the new broad bands present at 3012-3648 cm^{-1} range are due to the stretching vibration (υ_{OH}) of the coordinated water molecules. The stretching vibrational band of the active methylene group CH_2 in o-phenylenediamine present at 3181 cm^{-1} in the free diamine suffers lower frequency shift on complexation process and was found at 2961-3210 cm^{-1} due to departure from idealized symmetry on complex formation. Also a new set of bands in the IR spectra of the macrocomplex appear within the range 3012-3217 cm^{-1} which is due to the stretching vibration of the CH_3 group of acetylacetone moiety. The metal to nitrogen bonds (υ_{M-N}) give rise to a medium-strong bands at 370-490 cm^{-1}. Accordingly, metal ions will catalyze the template reaction between acetylacetone and o-phenylenediamine leading to the formation of macrocomplex molecule having the mode of bonding as follow:-

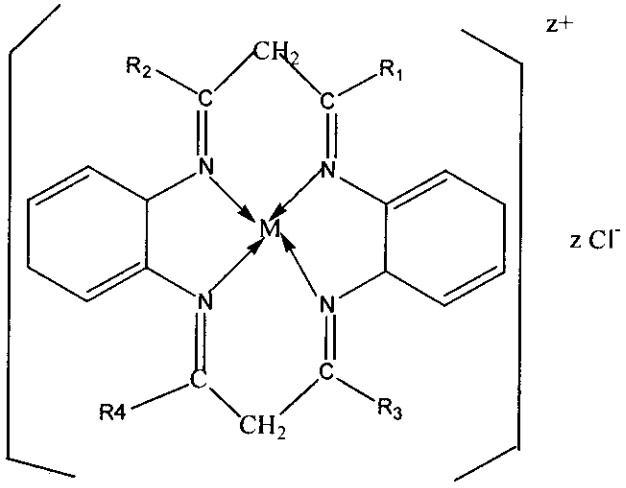

1- $R_1=R_2=R_3=R_4=CH_3$

2- $R_1=R_3=CH_3$, $R_2=R_4=Ph$

3- $R_1=R_2=R_3=R_4=Ph$

M = Fe^{3+}, Co^{2+}, Ni^{2+} and Cu^{2+}

4.ii. IR spectra of macrocyclic complexes formed between p-phenylene-diamine and acetylacetone, benzoylacetone and dibenzoylmethane:

The IR spectra of Fe^{3+}, Co^{2+}, Ni^{2+} and Cu^{2+} macrocyclic complexes of p-phenylenediamine with acetylacetone, benzoylacetone and dibenzoylmethane are studied and compared to those of the free organic compounds.

The spectra are recorded in Figs. (9-11) and the data are listed in Table (4). Inspection of the IR spectra reveals the following:-

(1) The strong absorption bands due to the stretching vibration of the C=O groups of the diketone molecules present originally at 1596-1600 cm^{-1} disappeared after complexation reaction as a result of azomethine bond formation.

(2) The stretching vibration band of NH_2 group present at 3373 cm^{-1} in the p-phenylenediamine moiety also disappeared

(3) The stretching vibration bands of the active methylene group (υ_{CH2}) of the diketone moiety suffer a shift toward lower frequency side as a resulting of electron delocalization due to complex formation.

(4) A new two sets of strong absorption bands within the ranges 1609-1657 and 1111-1219 cm^{-1} appear in the spectra of the macrocyclic complexes. These bands are due to the symmetric and asymmetric stretching vibration of the C=N group. The lower wave numbers at which these bands appear are may due to the participation of the N atom of the azomethine group in coordinate bond formation. This is supported by the appearance of new bands in the far IR region (372-496 cm^{-1}) due to υ_{M-N}.

(5) The presence of coordinated water molecules are confirmed by the presence of broad bands around 3500 cm^{-1} due to the stretching (υ_{OH}) of the OH group. The coordinated nature of

water molecules is confirmed by the appearance of the rocking mode of medium intensity at 818-829 cm^{-1} [66] and the bending vibrational mode (δ_{OH}) present in the 1300-1310 cm^{-1} range. In the light of these finding, the mode of bonding in the present complexes can be viewed as:

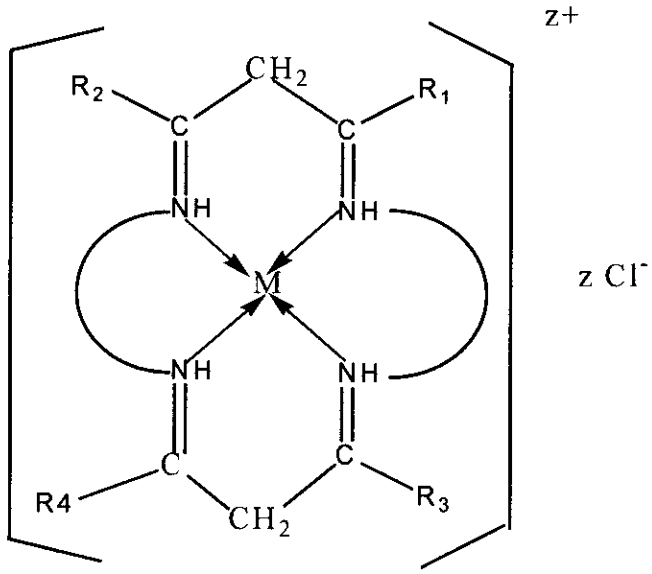

1- $R_1=R_2=R_3=R_4=CH_3$

2- $R_1=R_3=CH_3$, $R_2=R_4=Ph$

3- $R_1=R_2=R_3=R_4=Ph$

M = Fe^{3+}, Co^{2+}, Ni^{2+} and Cu^{2+}

Table (3): Main FT-IR frequencies (cm^{-1}) for macrocyclic complexes of o-phenylenediamine with acetylacetone, benzoylacetone and dibenzoyl methane.

Compounds	υ_{NH2}	υ_{OH}	δ_{OH}	Roc. OH	$\upsilon_{C=O}$	υ_{CH2}	υ_{sym} C=N	υ_{asym} C=N	υ_{M-N}	υ_{CH3}
o-phenylenediamine	3362	-	-	-	-	-	-	-	-	-
Acetyl acetone	-	-	-	-	1600	3181	-	-	-	2950
Benzoyl acetone	-	-	-	-	1598	2286	-	-	-	2286
Dibenzoylmethane	-	-	-	-	1596	2280	-	-	-	-
Fe(o-phen-acac)	-	3283	1276	821	-	2968	1602	1162	461	3217
Fe(o-phen-Benac)	-	3570	1261	817	-	2974	1651	1144	472	3102
Fe(o-phen-dbmeth)	-	3336	1311	828	-	2845	1659	1179	490	-
Co(o-phen-acac)	-	3210	1274	809	-	3210	1624	1114	433	3210
Co(o-phen-Benac)	-	-	1291	889	-	3059	1625	1113	429	3059
Co(o-phen-dbmeth)	-	3316	1308	833	-	2595	1595	1226	395	-
Ni(o-phen-acac)	-	3012	1292	812	-	2961	1624	1219	427	3012
Ni(o-phen-Benac)	-	3528	1290	808	-	2977	1624	1217	427	3122
Ni(o-phen-dbmeth)	-	3648	1307	821	-	2951	1652	1149	422	-
Cu(o-phen-acac)	-	3157	1308	843	-	3007	1606	1142	370	3175
Cu(o-phen-Benac)	-	3369	1285	809	-	2819	1623	1217	428	3012
Cu(o-phen-dbmeth)	-	3292	1307	840	-	2595	1595	1228	372	-

acac: acetylacetone, **o-phen:** o-phenylenediamine , **Benac:** Benzoylacetone , **dbmeth:** dibenzoylmethane.

Table (4): Main FT-IR frequencies (cm^{-1}) for macrocyclic complexes of p-phenylenediamine with acetylacetone, benzoylacetone and dibenzoyl methane.

Compounds	υ_{NH2}	υ_{OH}	δ_{OH}	Roc. OH	$\upsilon_{C=O}$	υ_{CH2}	υ_{sym} C=N	υ_{asym} C=N	υ_{M-N}	υ_{CH3}
p-phenylenediamine	3373	-	-	-	-	-	-	-	-	-
Acetyl acetone	-	-	-	-	1660	3181	-	-	-	2950
Benzoyl acetone	-	-	-	-	1598	2286	-	-	-	2886
Dibenzoylmethane	-	-	-	-	1596	2280	-	-	-	-
Fe(p-phen-acac)	-	3361	1307	826	-	2545	1622	1117	495	2847
Fe(p-phen-Benac)	-	3376	1297	827	-	2545	1510	1204	496	2845
Fe(p-phen-dbmeth)	-	3394	1273	818	-	2369	1628	1209	493	-
Co(p-phen-acac)	-	3358	1305	827	-	2549	1613	1111	496	2839
Co(p-phen-Benac)	-	3415	1307	826	-	2545	1625	1111	497	2826
Co(p-phen-dbmeth)	-	3378	1310	827	-	2548	1657	1112	426	-
Ni(p-phen-acac)	-	3292	1303	821	-	2566	1609	1180	372	2914
Ni(p-phen-Benac)	-	3263	1308	824	-	2550	1621	1192	495	2880
Ni(p-phen-dbmeth)	-	3460	1307	826	-	2546	1657	1184	431	-
Cu(p –phen-acac)	-	3295	1304	829	-	2849	1610	1157	395	2849
Cu(p-phen-Benac)	-	3069	1300	824	-	2849	1619	1219	465	2850
Cu(p- phen-dbmeth)	-	3324	1304	827	-	2850	1657	1170	490	-

acac: acetylacetone, **p-phen:** p-phenylenediamine, **Benac:** Benzoylacetone, **dbmeth:** dibenzoyl methane

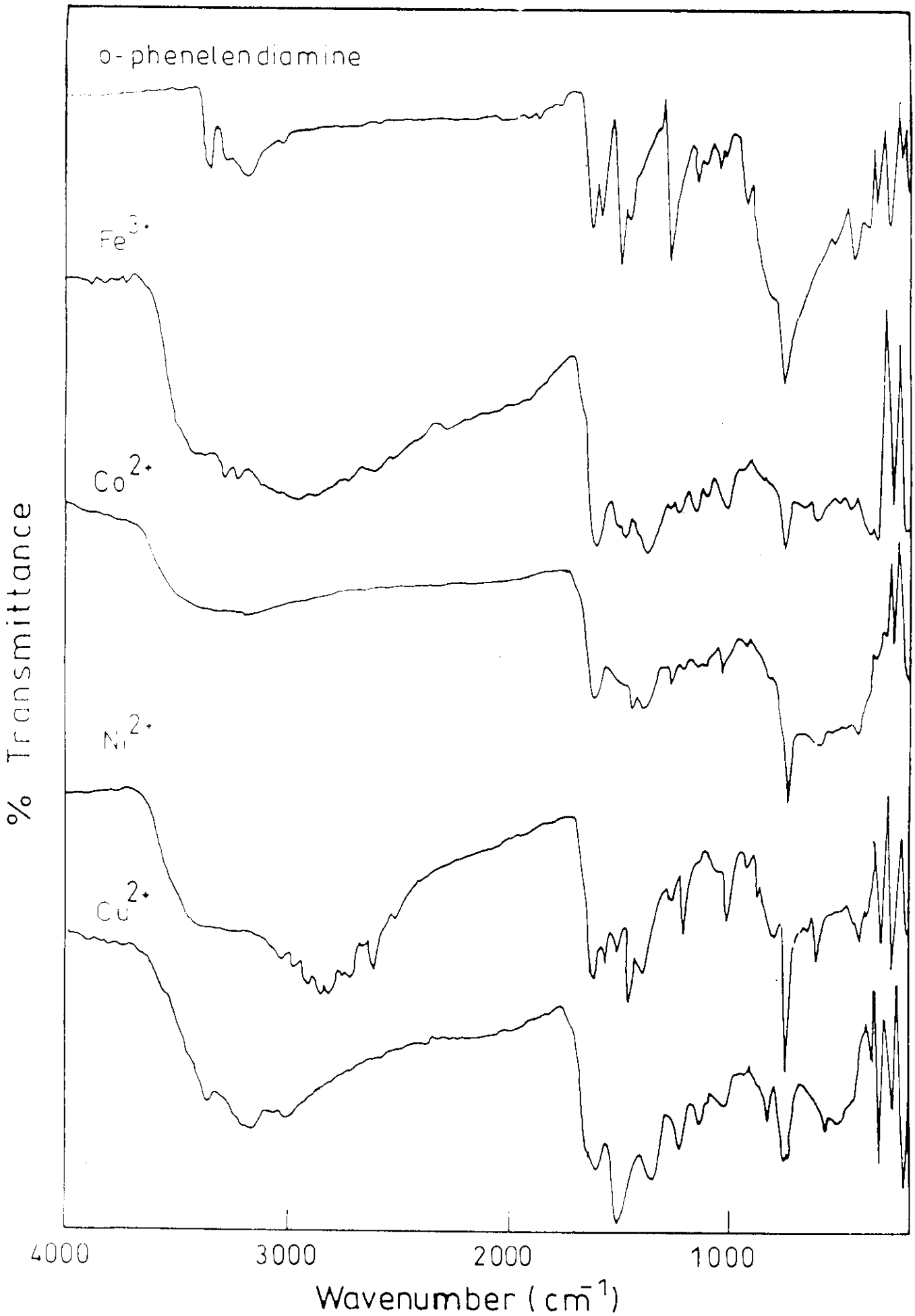

Fig (6) IR spectra of Fe^{3+}; Co^{2+}; Ni^{2+} and Cu^{2+} complexes with o-phenylene diamine and acetylacetone.

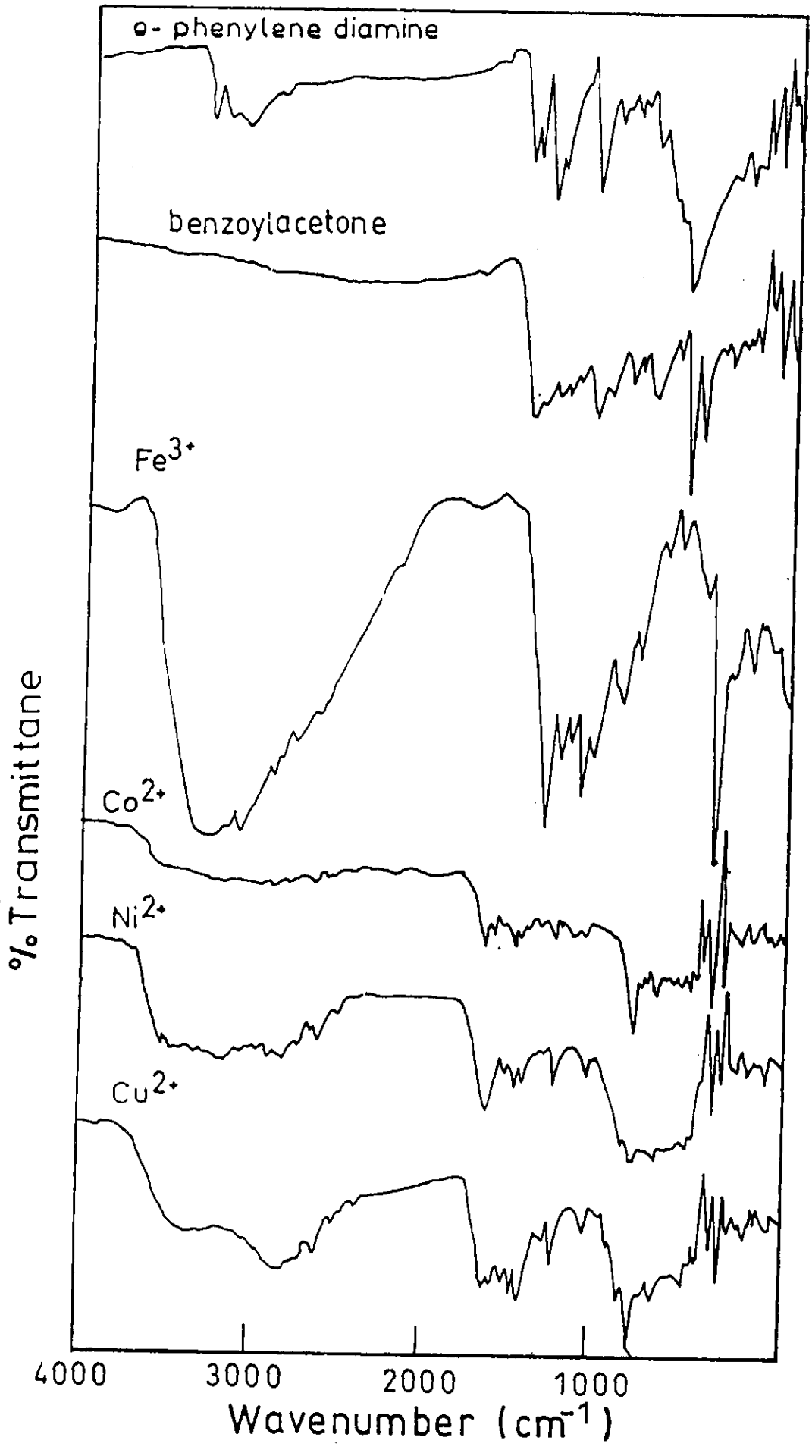

Fig.(7): IR spectra of Fe^{3+}, Co^{2+}, Ni^{2+} and Cu^{2+} complexes with o-phenylenediamine and benzoylacetone.

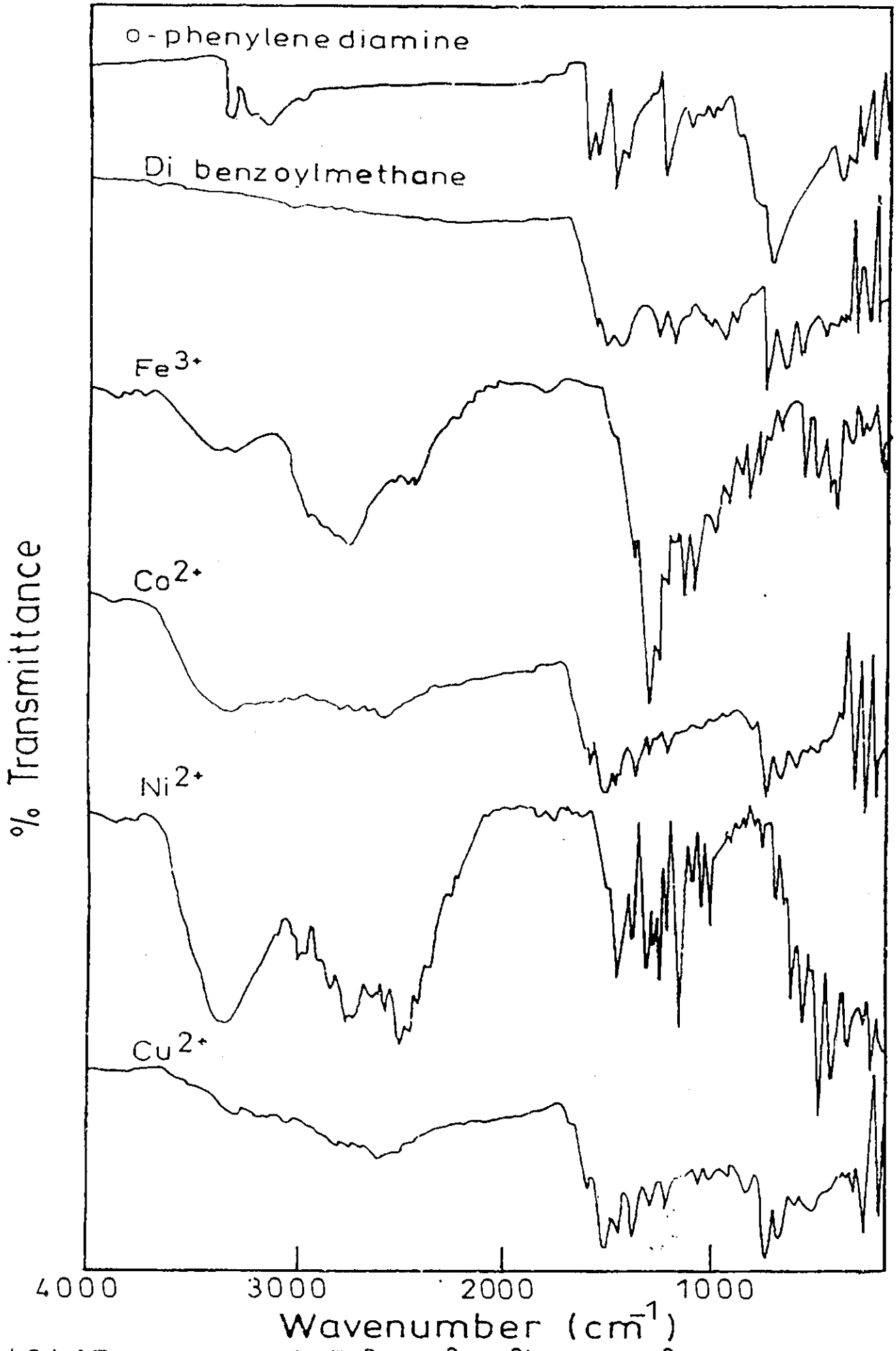

.(8): IR spectra of Fe^{3+}, Co^{2+}, Ni^{2+} and Cu^{2+} complexes with o-phenylenediamine and dibenzoylmethane.

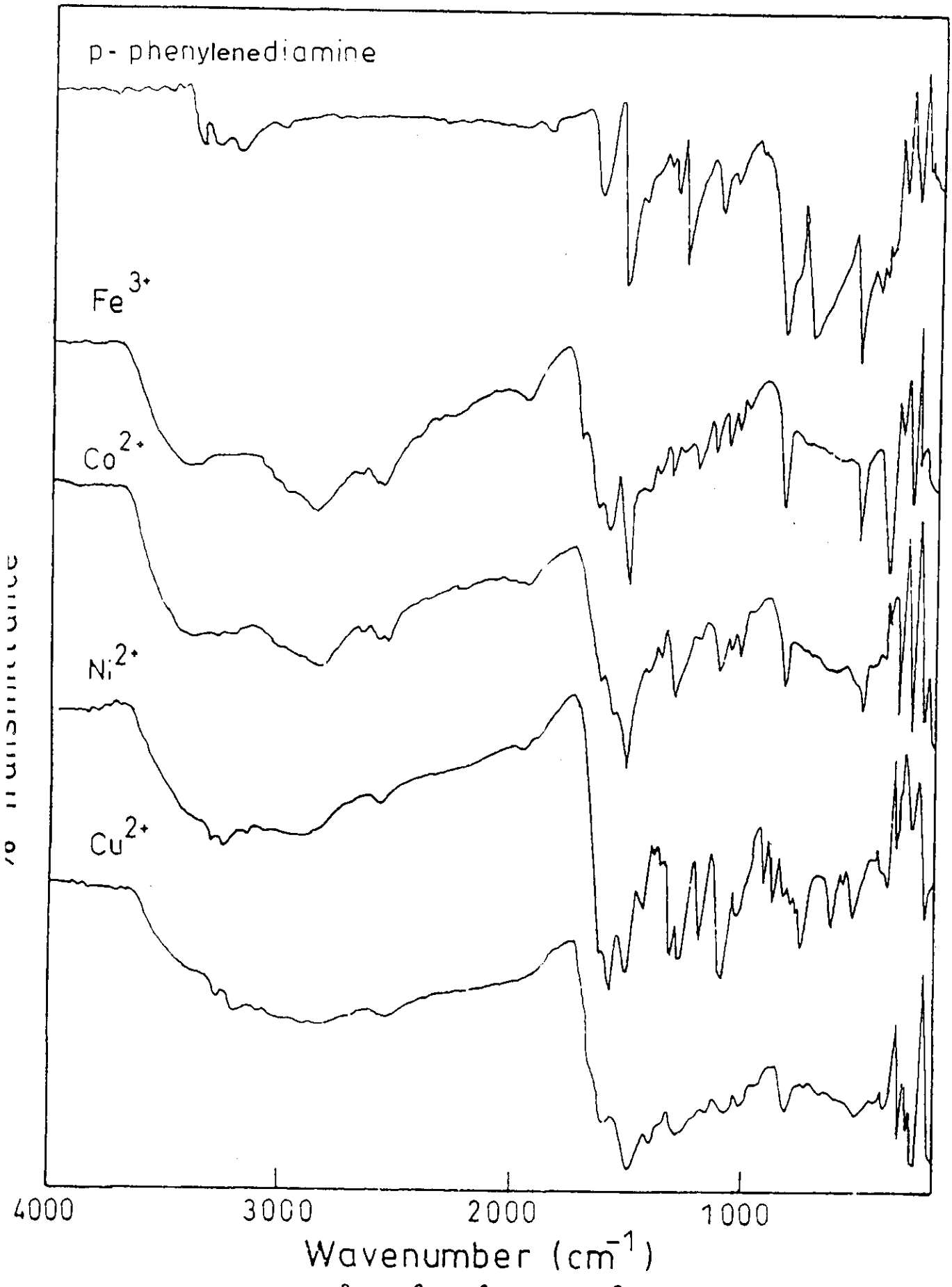

ig. (9): IR spectra of Fe^{3+}, Co^{2+}, Ni^{2+} and Cu^{2+} complexes with p-phenylene diamine and acetylacetone.

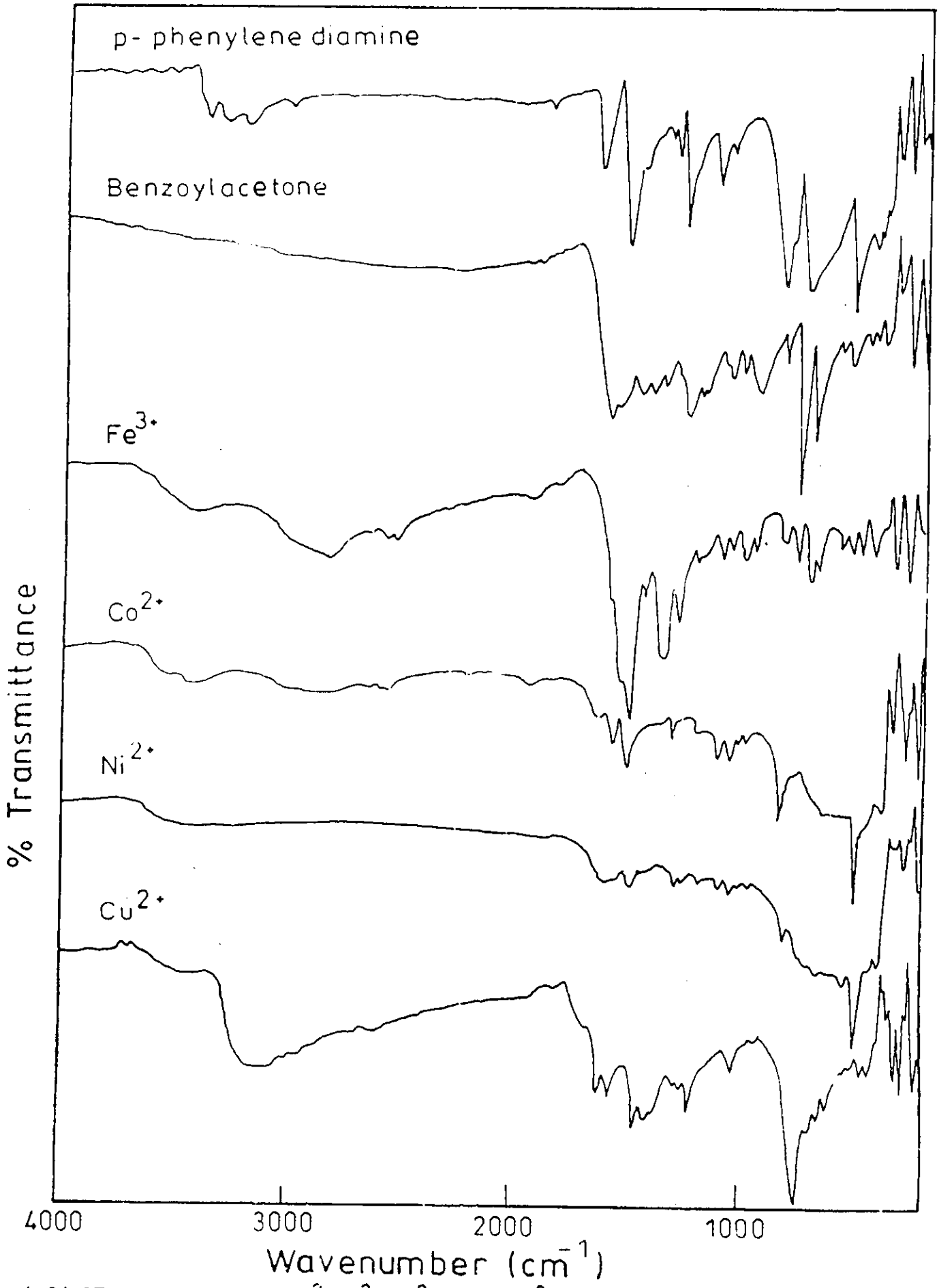

Fig.(10): IR spectra of Cu^{2+}, Ni^{2+}, Co^{2+} and Fe^{3+} complexes with p-phenylene-diamine and benzoylacetone.

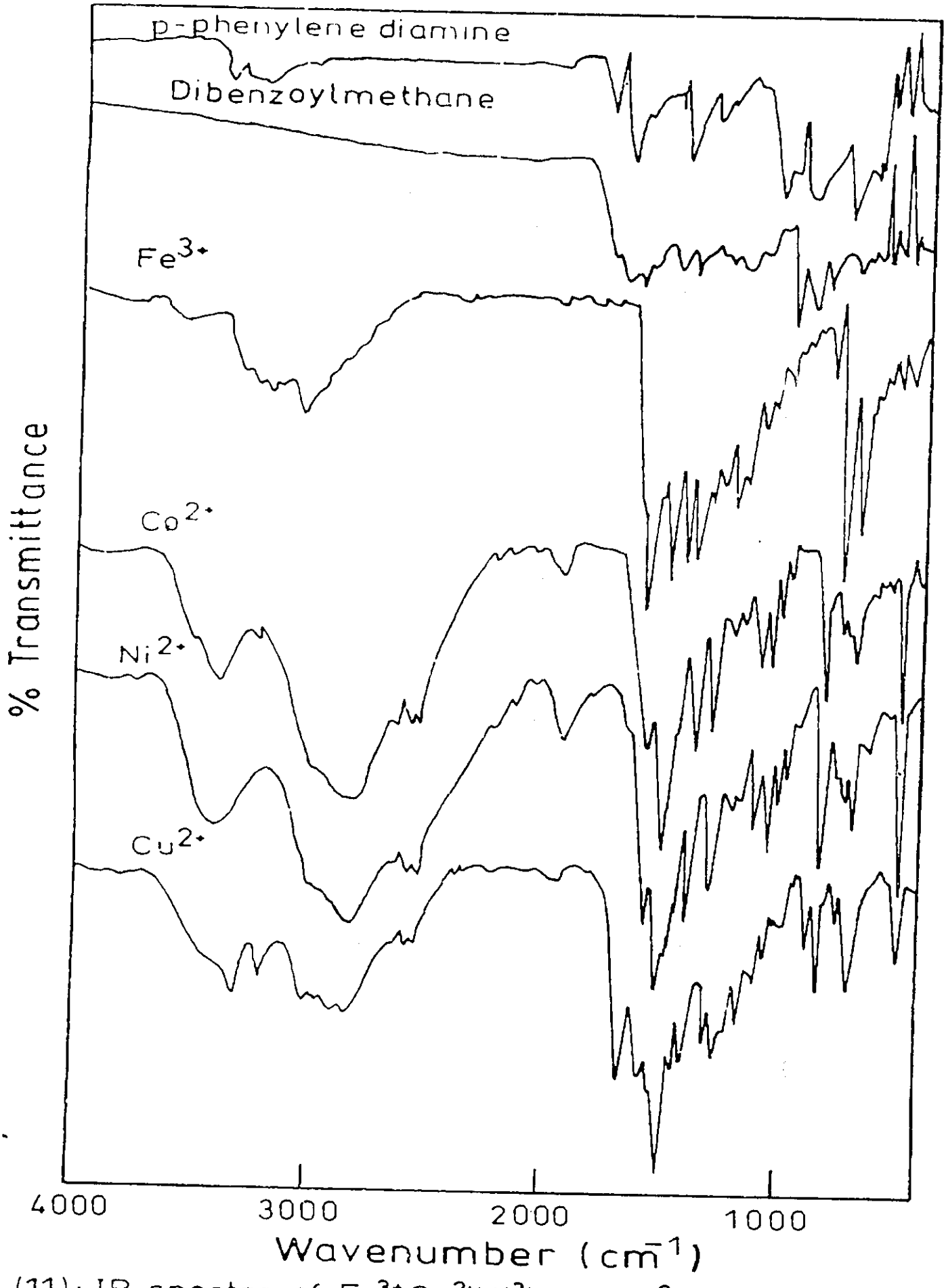

g. (11): IR spectra of Fe^{3+}, Co^{2+}, Ni^{2+} and Cu^{2+} complexes with p-phenylene diamine and dibenzoylmethane.

5. Electronic spectra and magnetic properties of solid complexes theory

Considerable emphasis and importance has placed upon the determination of magnetic properties of transition metal complexes [67-69] such studies have contributed much to our understanding of the chemistry as well as the characterization of these compounds, particularly in regard to oxidation states, stereo chemistry of the central atoms and their bond types.

5.1. Energy-level diagrams

In order to interpret the spectra of the complexes, we must employ an energy–level diagram based upon the Russell-Saunders states of the relevant d^n configuration in the free (uncomplexed) ion. It can be shown that, just as the set of the five *d* orbitals is split by the electronic field of surrounding ligands to give two or more sets of lower degeneracy, this applies to the various Russell-Saunders states of a d^n configuration too. For example, in the absence of external forces, the set of the five *d* orbitals is degenerate, the ground state of a d^1 ion is ^2D, and the electron has an equal probability of being in any of the five *d* orbitals. Under the influence of an octahedral field, degenerate orbitals are split into $t_{2g}^{\ 1}$ and $e_g^{\ 0}$ orbitals and, likewise, the ^2D state is split into a $^2T_{2g}$ state (representing the $(t^1_{2g}\ e^0_g)$ configuration) and a ^2E_g state (representing the $(t^0_{2g}\ e^1_g)$ at higher energy.

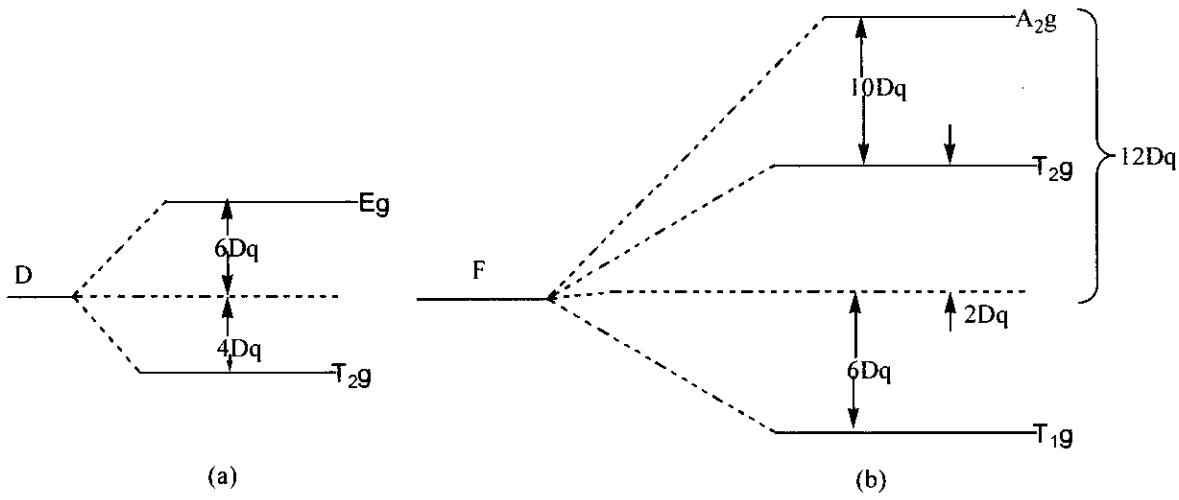

Fig.(5-1): Spilitting of terms arising from (a) d^1 and (b) d^2 electronic configurations

The ligand field theory allows orbital overlap involving all parameters of interelectronic interactions as variables instead of them equal to the values found for the free ions. Of these parameters, two are of decisive importance, namely, the spin orbit coupling constants and the interelectronic repulsion parameters, which may be used as the Salter Condon F_n parameters or as certain linear combinations of these called the Racah parameters, B and C [70] which are usually more convenient.

- The spin orbital coupling constant (λ) plays a considerable role in determing the detailed magnetic properties of many ions in their complexes, for example the deviations of some actual magnetic moments from spin-only values and inherent temperature-dependence of some moments. All studies to date show that in ordinary complexes the values of (λ) are 70-85% of those the free ions.
- The Racah parameters are measures of the interelectronic repulsion responsible for the differences in energy between the various Russell-Saunders states of an atom. These are linear combinations of

certain coulomb and exchange intergrals. The energy differences between states of the same multiplicity are, in general, multiples of B only, where as the differences between states of different multiplicity are expressed as sums of multiplies of both B and C. They are related by the equations [71].

$$B = F_2 - 5F_4$$

$$C = 35\ F_4$$

And the energy separation between the ground term ^nF, and the excited term ^nP, is 15B [72].

Since the wave functions for these two states (^4F and ^4P) have identical symmetry, they will mix and the moment of mixing will be inversely proportional to the difference in energy between the ^4F and ^4P levels, Fig. (5-3). As a result of the mixing the $^4T_{1g}(F)$ will lie some what lower in energy, and the $^4T_{1g}(P)$ will lie some what higher in energy than they would, if mixing had not occurred. As shown in Fig. (5-2) the difference between the ^4F and ^4P states in the free ion is 15 B.

For most transition metal ions B can be estimated as approximately 1000 cm^{-1} and C= 4B for the free ion[72].

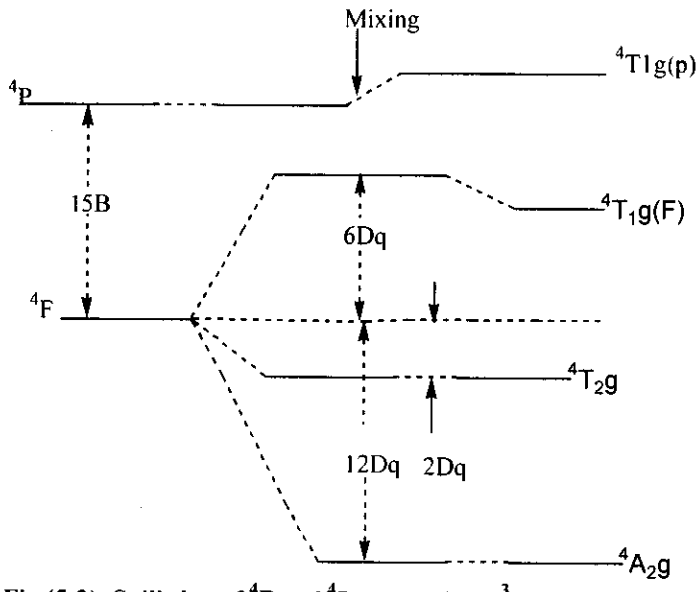

Fig.(5-2): Spilitting of ^4F and ^4P terms of a $3d^3$ ion in octahedral fields illustrating the inversion of and mixing of the T_{1g} terms(right).

5.2. Nephelauxetic effect

The value of B in complexes is always smaller than that of the free ion. The phenomenon is known as the nephelauxetic effect and is attributed to delocalization of the metal electrons over molecular orbitals that encompass not only the metal but the ligands as well. It is found that the electron-electron repulsion in complexes is somewhat less than in the free ion. The decrease of electron-electron repulsion may be attributed to an increase in the distance between electrons and hence, to an effective increase in the size of the distance between electrons and hence, to an effective increase in the size of the orbitals (nephelauxetic means "cloud expanding"). This increase apparently results from the combination of orbitals on the metal and ligand to form larger molecular orbitals through which the electrons can move. Ligands which can delocalize the metal electron over a large space (those containing larger atoms with *d* orbitals) are most effective in this manner.

As a result of this delocalization or "cloud expanding" the average interelectronic repulsion is reduced and B^{-}(representing B in complex) is smaller. The nephelauxetic ratio, β, is given by:

$$\beta = \bar{B} / B$$

Estimates [72] of β may be obtained from the nephelauxetic parameters h_x for the ligand and K_M for the metal:

$$(1-\beta) = h_x . K_M$$

In octahedral geometry, if all three transitions are observed,

$$\nu_1 \; ; \; A_{2g} \longrightarrow T_{2g}$$

$$\nu_2 \; ; \; A_{2g} \longrightarrow T_{1g}(F)$$

$$\nu_3 \; ; \; A_{2g} \longrightarrow T_{1g}(P)$$

It is a simple matter to assign a value to $\overline{B}$ since the following equation must hold

$$\bar{B} = \nu_3 + \nu_2 - 3\nu_1$$

5.3. Stereochemistry

In a free ion the *d* orbitals are degenerate. When the ion is placed into a molecular environment, this degeneracy will be lifted at least partially, the relative energies of the *d* orbitals, and therefore the electronic spectrum, will depend upon the stereochemistry concerned.

- Octahedral complexes

The x, y and z axis of a regular octahedron are equivalent, so that it is therefore impossible to distinguish between the dxz, dxy and dyz orbitals and also between the d_x^2-$_y^2$ and d_z^2 orbitals. It follows that the *d* orbitals in an octahedral environment will split into two levels, the triply degenerate t_{2g} (d_{xz} , d_{yz} and d_{xy}) and doubly degenerate e_g (d_x^2-$_y^2$ and d_z^2) levels.

Since the e_g orbitals point directly towards the ligands whilst the t_{2g} orbitals point between them, the energy order will $t_{2g} < e_g$. The extent, to which the e_g and the t_{2g} orbitals are separated is donated by the quantity 10Dq.

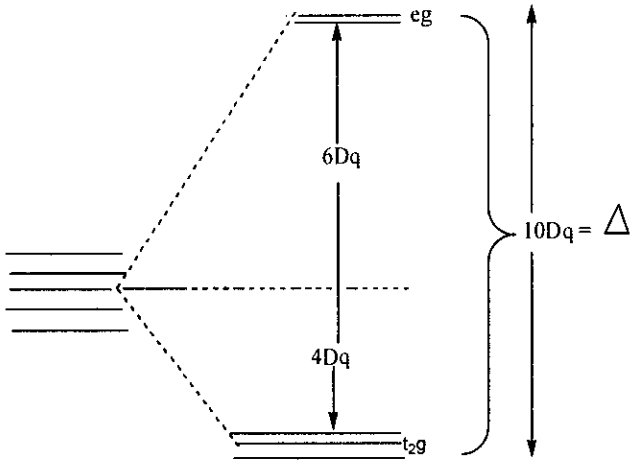

Fig.(5-3): Spilitting of the degenercy of the five d orbitals by an octahedral ligand field.

- Tetrahedral complexes

Two of the most common geometries for 4-coordinate complexes are the tetrahedral and square planar arrangements. Tetrahedral coordination is closely related to cubic coordination.

In this arrangements, the ligands do not directly point to any of the metal *d* orbitals, but they come closer to the t_2 (d_{xz}, d_{yz}, and d_{xy}) orbitals directed to the edges of the cube than to the e ($d_{x^2-y^2}$ and d_{z^2}) orbitals directed to the center of the faces of the cube, (The g subscripts are dropped since a tetrahedron does not have a center of symmetry). Hence, the t_2 levels are raised in energy and the e levels stabilized. Again, the principle of constant energy holds i.e. the t_2 levels are raised 4 Dq and e levels are lowered 6 Dq compared with the undisturbed *d* levels, the through the overlap amount of splitting is only 4/9 of an octahedral field with identical ligands Fig. (5-4).

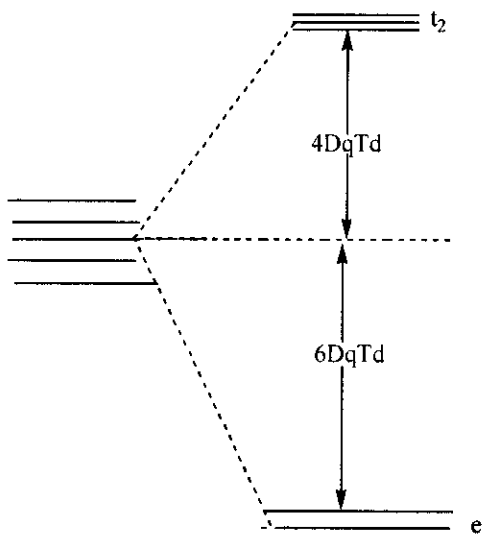

Fig.(5-4): Spilitting of d orbitals in a tetrahedral field.

- Tetragonal and square planar coordination

The square planar arrangement is a special case of the more general D_{4h} symmetry involving tetragonal distortion of octahedral complexes. Fig. (5-5).

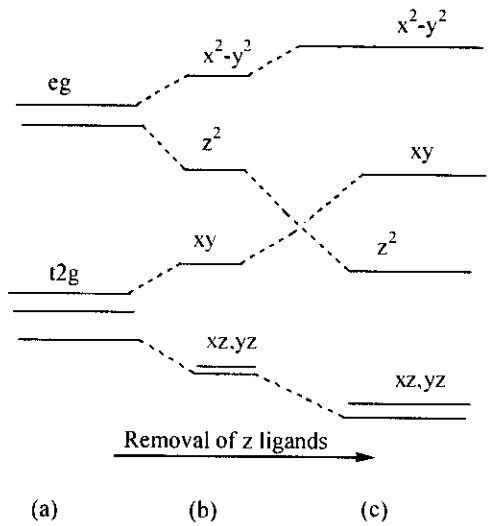

Fig.(5-5): Distortion of octahedral complex through (a) tetragonal symmmetry (b) to square planar limit. (c) The orbital may lie below the xz and yz orbital in the square planar complex.

Consider what happens to the energy levels as the ligands along the z axis are withdrawn. As the distance of the z charges from the metal increases, the repulsion of the dz^2 and d_{yz}, d_{xz} will decrease the former orbital in energy more sharply than the latter pair.

If the ligands on the z axis are removed to infinity, a square planar arrangement is obtained. The removal of the z charge affects the dx^2-y^2 and d_{xy} orbitals to the same extent since, considering the symmetry along the z axis, the two orbitals are equivalent, and therefore they maintain their separation of 10 Dq.

Metal ions having a d^8 configuration and ligands exerting a large field effect favor square planar complexes. This combination will result in low spin complexes with the d^8 electrons occupying the low energy d_{xz}, d_{yz} (degenerate), dz^2 and d_{xy} orbitals, while the high energy dx^2-y^2 orbital

remains unoccupied. The stronger the ligand field the higher will the dx^2-y^2 orbital be raised above the d_{xy} level.

- ***Electronic spectra***

Most of the complexes of the transition elements are highly coloured compounds, which mean that they are capable of absorbing radiant energy in the visible region of the spectrum. Indeed, studies of the absorption spectra of these compounds reveal, that they absorb energy in the infrared (IR) and ultraviolet (UV) regions as well as in the visible. The study of electronic absorption spectra of transition element compounds can be evaluate the stereochemistry of the transition metal chelates.

First, we can list four general types of electronic transitions that may be observed with *d*-element complexes:

1- Transitions may occur between the split *d* levels of the central atom, giving rise to the so-called *d-d* or ligand field spectra. The spectral region, where these bands occur the near IR, visible, and UV, and thus the transitions are the ones primarily responsible for the great variety of colour found in transition element complexes. In practice the region generally scanned is 10000 to 30000 cm^{-1}, although some *d-d* transitions occur beyond both ends of this range. However, the lower frequencies are often not accessible experimentally, and the higher frequencies, which are accessible, generally to 50000 cm^{-1} are almost invariably covered by much more intense charge transfer and/or intraligand transitions.

2- Transitions may occur from molecular orbitals located primarily on the ligands, the metal-ligand bonding σ or π molecular orbital, to nonbonding or antibonding molecular orbitals located primarily on the metal atom Fig. (5-6). Such transitions are called ligand to metal charge

transfer (L-M) transitions. It is clear, that for octahedral complexes four basic classes of absorption bond may be expected, viz.

υ_1	π	-	$t_{2g}(\pi^*)$	
υ_2	π	-	$e_g(\sigma^*)$	
υ_3	σ	-	$t_{2g}(\pi^*)$	
υ_4	σ	-	$e_g(\sigma^*)$	in order of increasing energy

In a sense, the energy of such of electronic transitions reflected the thermodynamic tendency for a redox reaction, specifically the reduction of the central ion by the ligand.

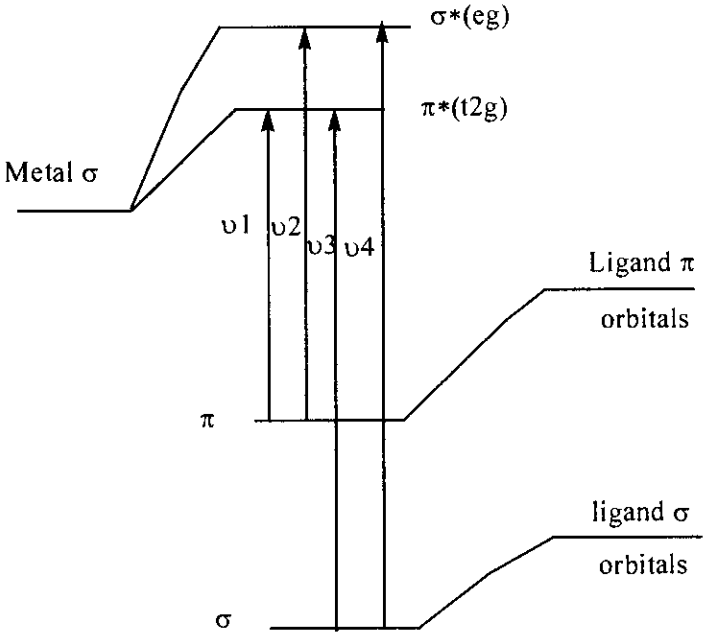

Fig.(5-6): Partial MO diagram for an octahedral MX_6 complex, showing the four main classes of L- M charge transfer transitions.

3- The transition which involve electrons being excited from nonbonding or antibonding arbitals located primarily on the metal atom to antibonding orbitals located primarily on the ligands are termed metal to ligand charge transfer (M-L) transitions. The bands generally occur in the UV region, but occasionally are found tailing off into or even peaking in the visible region.

4- The electronic transitions which involve electrons being excited from one ligand orbital into another ligand orbital. These intraligand transitions generally occur with energies found in the UV region and they are often little affected by coordination. In addition, their bands can usually be disentangled from the equally intense charge transfer bands in their neighborhood.

Next we must consider a second question, that concerning the expected probabilities or intensities of the various types of transition. This requires an examination of certain quantum mechanical properties possessed by the wave functions which represent the various eigenstates or energy levels.

1- The first rule states, that any transition in which $s \neq 0$ is forbidden, i.e. an allowed transition must be one in which the spin state of the complex does not change.

However, this spin selection rule is not completely valid in the presence of spin orbit coupling. Therefore, spin-forbidden bands do appear in the spectra of many transition metal complexes, but they are generally one to two orders of magnitude weaker than the spin-allowed bands, and their intensities increase with increasing spin-orbit coupling constant, where the latter increase in the orders : $d^1 < .. < d^9$ and $3d < 4d < 5d$.

2- The second rule is the Laporte selection rule: "In complexes with a center of symmetry the only allowed transition are those with a change of parity", i.e., gerade to ungerde $g \rightarrow u$ and $u \rightarrow g$ are allowed but not $g \rightarrow g$ and $u \rightarrow u$. Since all *d* orbitals have gerade symmetry this means that all *d-d* transitions in centrosymmetric molecules (octahedral symmetry being the most important example) are formally forbidden.

If any distortion occurs for the octahedron which alters bond lengths or bond angles, then the effective group to the molecule belongs not O_h but some lower symmetry group, which may not have a center of symmetry.

In practice, the most important mechanism by which the parity selection rule is relaxed in molecules with a center of symmetry is temporary removal of the center of symmetry by odd vibrations. If a molecule absorbs a quantum of radiation which excites an odd mode of vibration, the vibrationally excited molecule is not restricted by the parity rule and can now undergo a *d-d* transition. Such a mechanism is known as vibronic coupling (vibrational–electronic)[73], the electronic transition occurs with a simultaneous excitation of one or more vibrational modes. Tetrahedral complexes do not have a center of symmetry. Furthermore, ungerade, ungerade P orbitals can mix with d (d_{xy} ,d_{xz} and d_{yz}) orbitals to remove some of the "forbiddenness" from the Laporte rule.

5.4. Electronic spectra and magnetic properties of the investigated solid complexes:

The results of magnetic measurements (at room temperature) for Fe^{3+}, Co^{2+}, Ni^{2+} and Cu^{2+} macro complexes along with electronic absorption spectral data are listed in Table (5). The electronic spectra are shown in Figs. (14-21) and Figs. (12, 13) for ligands in nujol mull and DMF respectively. In general, the position of maximum absorptions in nujol mull show slight difference from those in DMF indicating different geometries in solid and solution states.

5.4.1. Spectra and magnetic properties of Fe^{3+} macrocyclic complexes

The room-temperature magnetic moments of Fe^{3+} complexes lie within the range 1.38-2.32 B.M. indicating low spin $(t_{29})^5$ electronic configuration. This will make *d-d* transitions spin-allowed and relatively broad. The electronic spectra of Fe^{3+}- macrocyclic complexes (*c.f* Figs. 14, 15) show two broad bands and a shoulder within the ranges: (13552 – 19205 cm^{-1}); (υ_1), (17637- 19841cm^{-1}) (υ_2) and (22026.26666 cm^{-1});(υ_3), which are assigned to the following transitions:

$$\upsilon_1 = {}^6A_{1g} \rightarrow {}^4T_{1g}$$

$$\upsilon_2 = {}^6A_{1g} \rightarrow {}^4T_{2g}\,(G)$$

$$\upsilon_3 = {}^6A_{1g} \rightarrow {}^4A_{1g},\ {}^4Eg$$

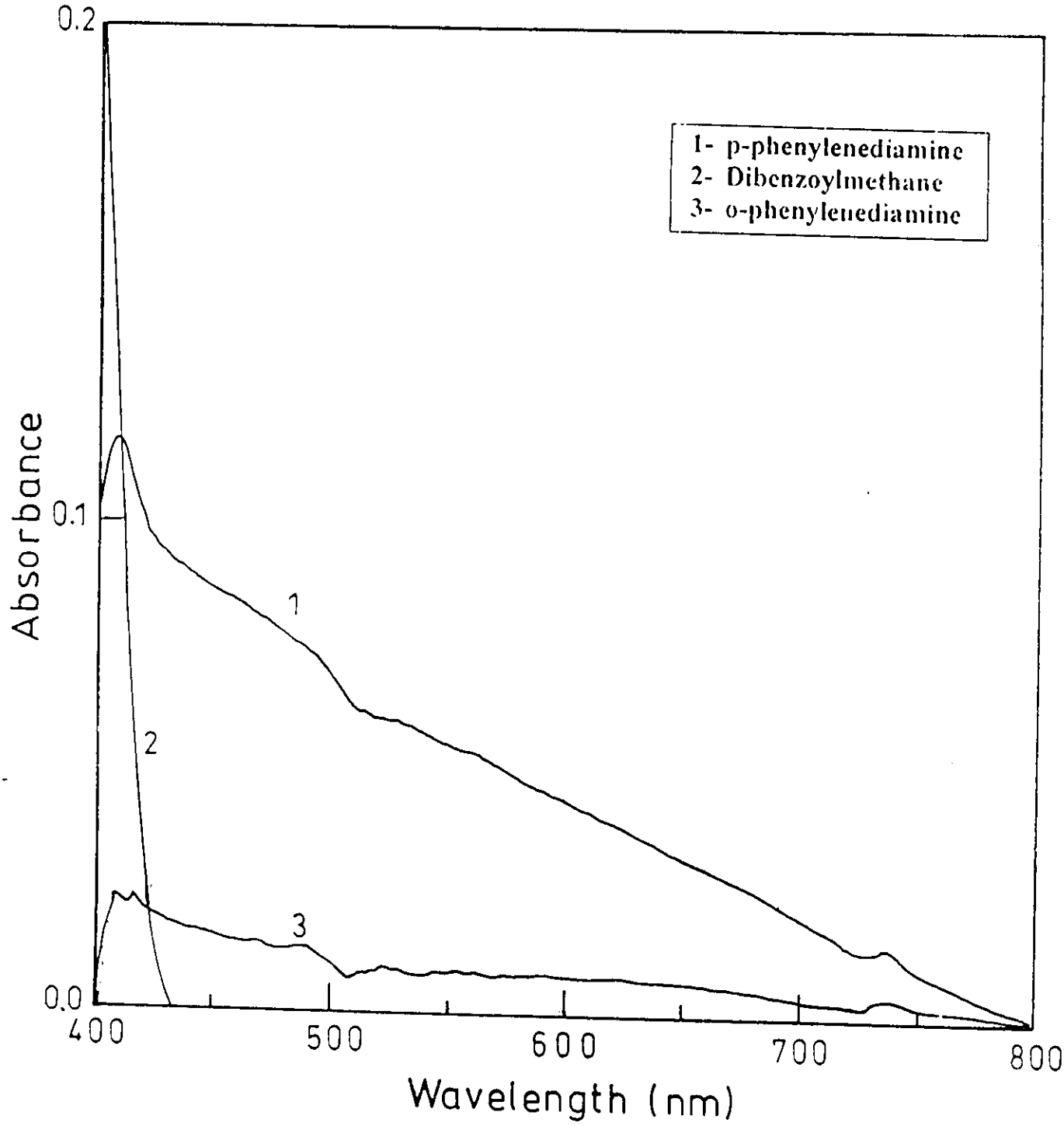

Fig.(12): Electronic absorption spectra of ligands in Nujol mull

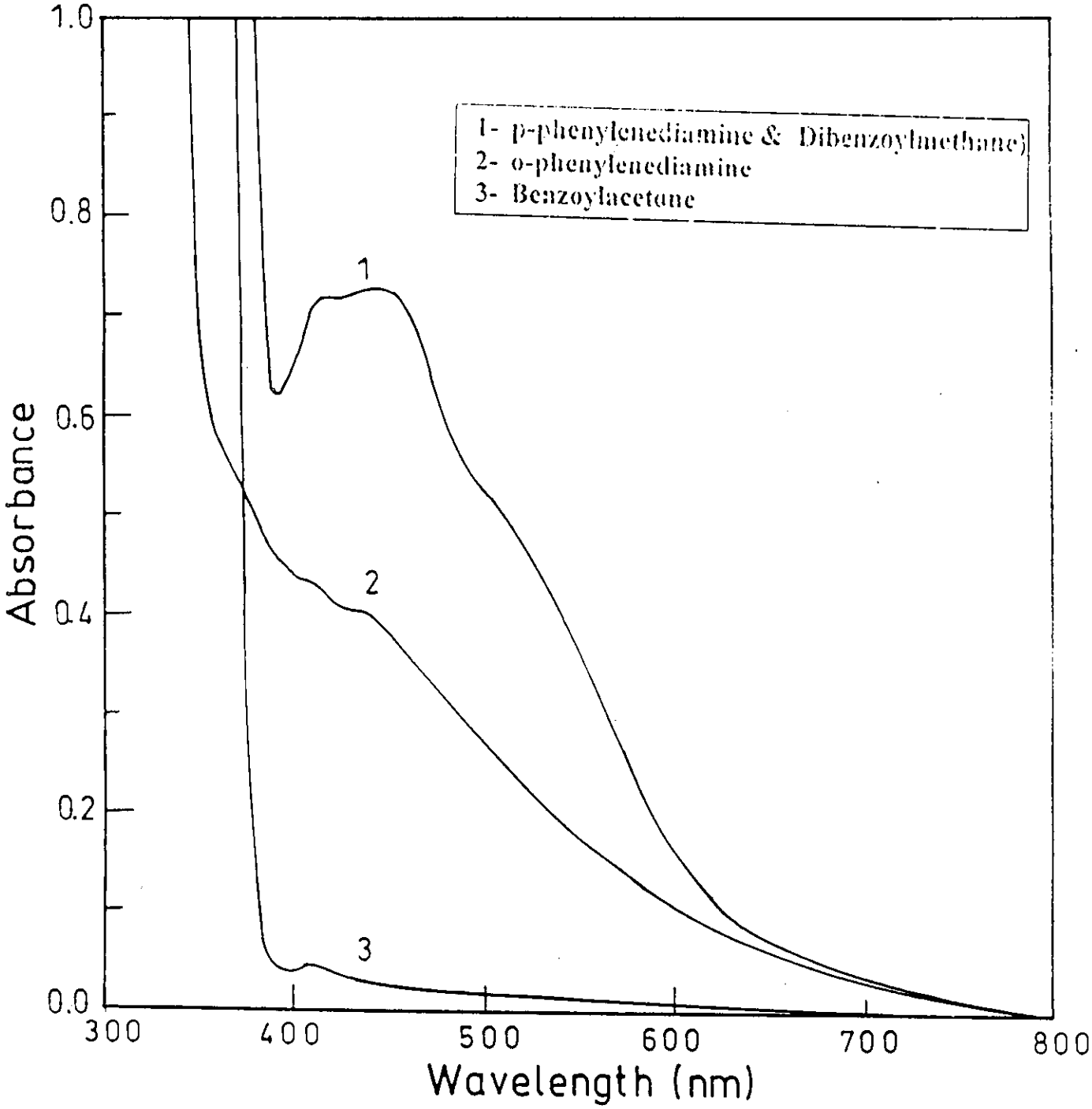

Fig.(13): Electronic absorption spectra of ligands in DMF

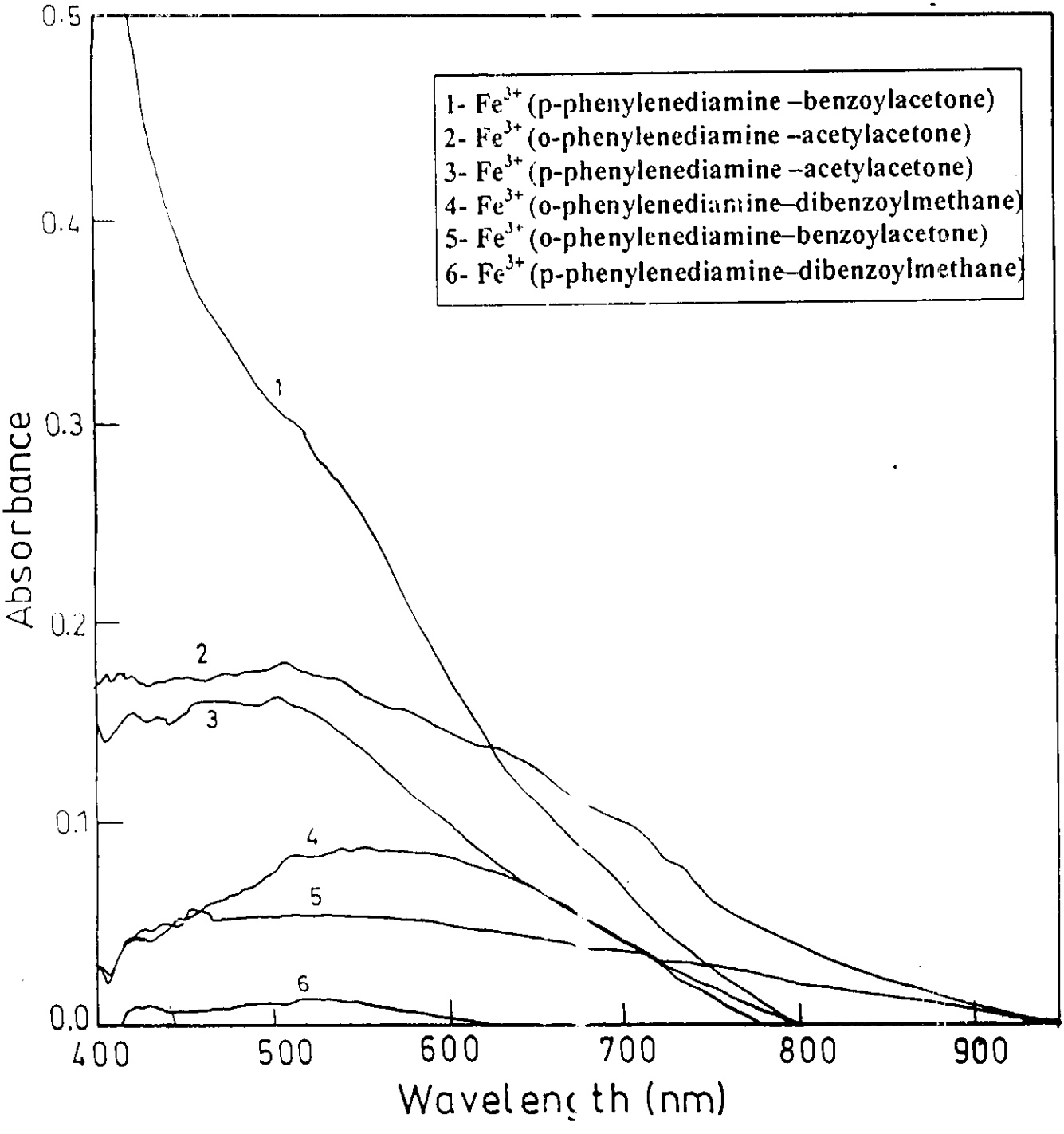

Fig. (14) Electronic absorption spectra of macrocyclic Fe^{3+} complexes in Nujul mull.

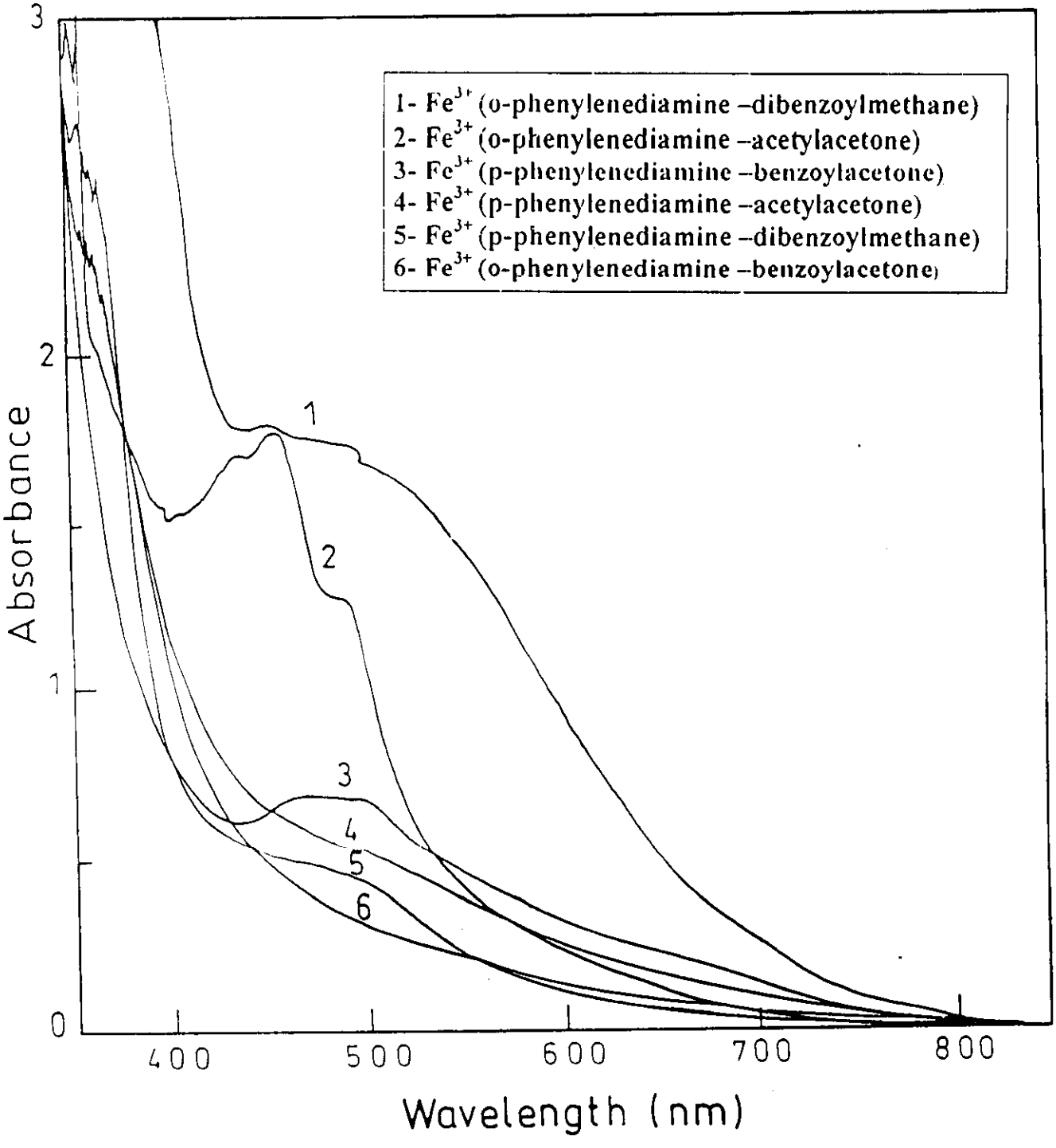

Fig. (15): Electronic absorption spectra of macrocyclic Fe^{3+} complexes in DMF

5.4.2. Spectra and magnetic properties of Co^{2+} macrocyclic complexes

For Co^{2+} complex and in octahedral environment, the following transitions are expected [74].

$$\upsilon_1 = {}^4T_{1g} \rightarrow {}^4T_{2g}$$
$$\upsilon_2 = {}^4T_{1g} \rightarrow {}^4A_{2g}$$
$$\upsilon_3 = {}^4T_{1g} \rightarrow {}^4T_{1g}\,(P)$$

From which the ligand field parameters (10Dq) and (B) can be calculated from the relation

$$\upsilon_1 = 5\,Dq - 7.5\,B + {}^1/_2(225\,B^2 + 100\,D_q{}^2 + 180\,D_qB)^{1/2} \qquad (1)$$
$$\upsilon_2 = 10\,Dq - 7.5\,B + {}^1/_2(225\,B^2 + 100\,D_q{}^2 + 180\,D_qB)^{1/2} \qquad (2)$$
$$\upsilon_3 = (225\,B^2 + 100\,D_q{}^2 + 180\,D_qB)^{1/2} \qquad (3)$$

The solid state electronic spectra (nujol mull) of Co^{2+} complexes of o-phenylenediamine with acetylacetone, benzoylacetone and dibenzoyl methane show two broad bands within the ranges 15026-51097 and 19712-23697cm^{-1} corresponding to ${}^4T_{1g} \rightarrow {}^4A_{2g}$ (ν_2) and ${}^4T_{1g} \rightarrow {}^4T_{1g}(P)$ (ν_3) transition respectively[75,76]. This indicates an octahedral environment around the Co^{2+} ions, this is supported by the values of magnetic moments measured at 298 K (Fig. 16,17) being in the range 2.45-3.27 BM expected for high spin octahedral field. The values of 10Dq and B are calculated from equation (1-3) and given in Table (5).

The magnetic moments of Co^{2+} macrocomplexes with p-phenylene-diamine with acetylacetone, benzoylacetone and dibenzoylmethane lie within the range (1.54-1.83 BM) which fall in the range reported for square-planar or low spin octahedral environments. However, the presence of a characteristic bonds at the vicinity of 20000 cm^{-1} suggest a square-planar configuration around the Co^{2+} ions in these cases [77].

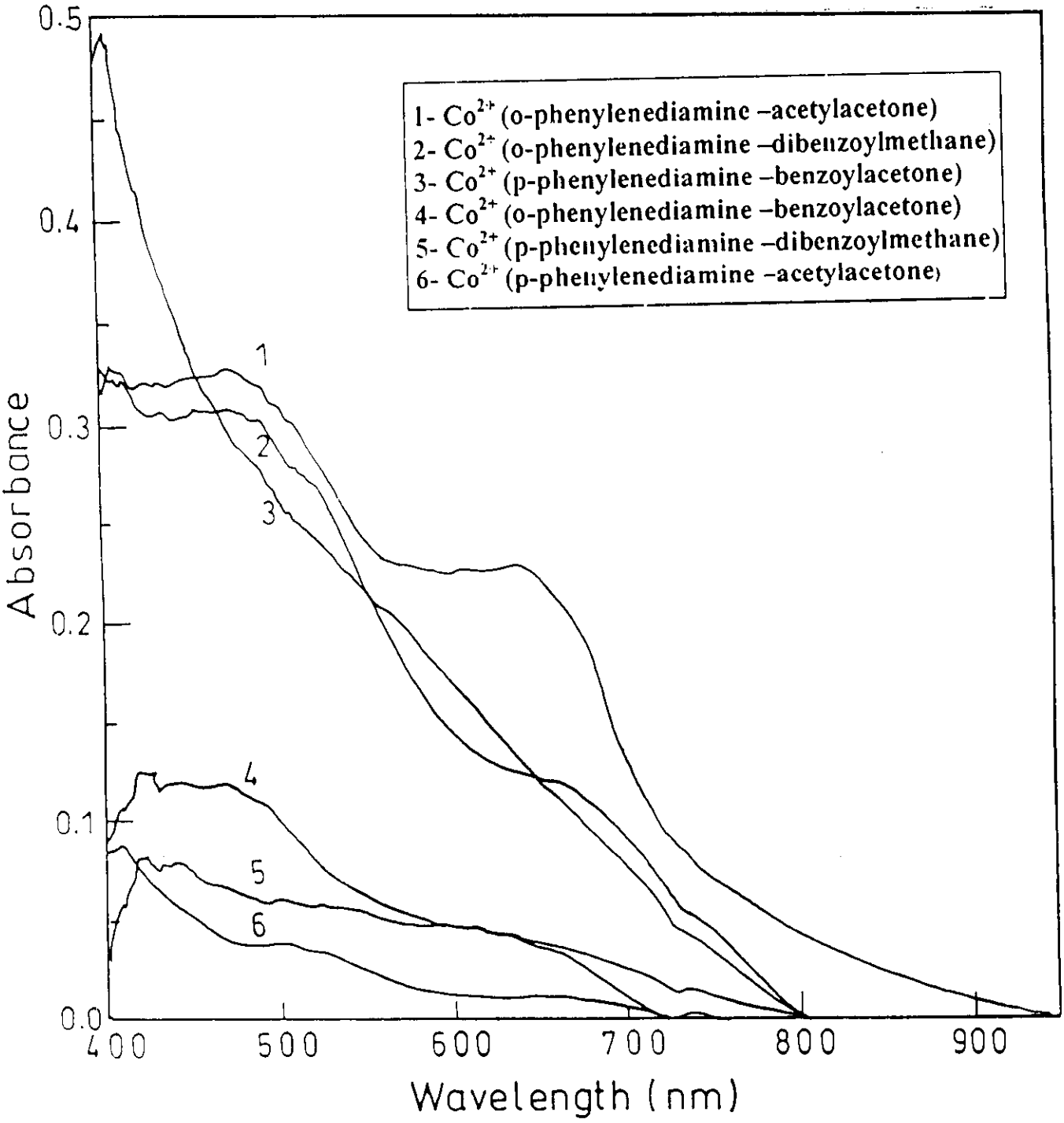

Fig. (16) : Electronic absorption spectra of macrocyclic Co^{2+} complexes in Nujul mull.

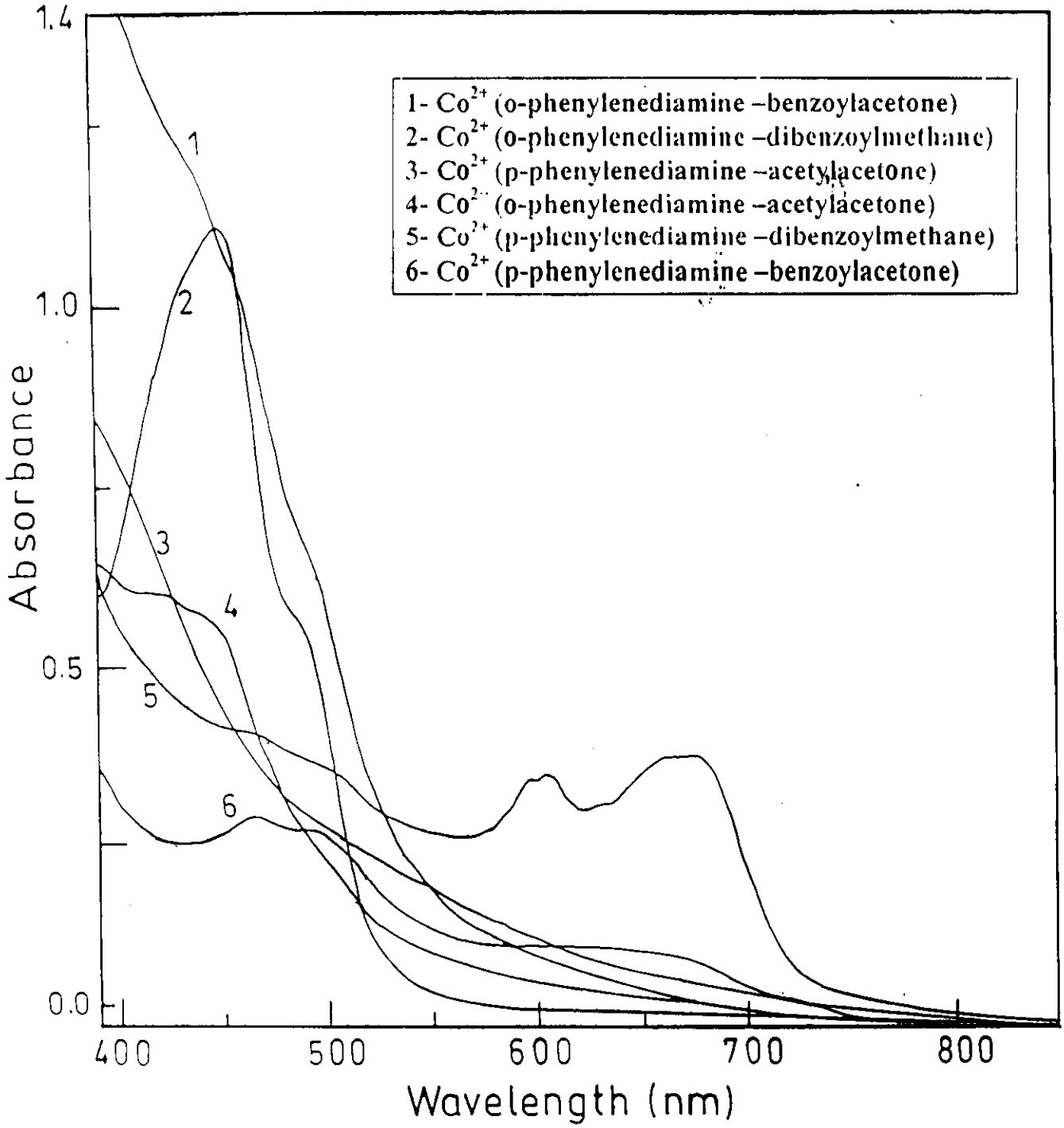

Fig. (17) : Electronic absorption spectra of macrocyclic Co^{2+} complexes in DMF.

5.4.3. Spectra and magnetic properties of Ni^{2+} macrocyclic complexes

Planar geometry is preferred for the majority of four-coordinated Ni^{2+} complexes. This is because the planar configuration makes one of the d-orbitals (namely d_{x2-y2}) of high energy and the eight electrons can occupy the other four d-orbitals leaving this strongly antibonding d_{x2-y2} vacant. So, the square-planar Ni^{2+} complexes are invariably diamagnetic and are characterized by the presence of medium intensity band in the range 20000-23500 cm^{-1} [73].

All the investigated Ni^{2+} complexes (Figs 18, 19) show diamagnetic behavior except those of o-phenylenediamine with acetylactone and dibenzoylmethane which showed paramagnetic character with μ_{eff} = 1.65 and 1.11 B.M. respectively. This suggests that those former complexes are of low-spin square planar geometry. The four coordination sites available for coordination are all occupied by electron pairs from the nitrogen atom of the tetraaza group.

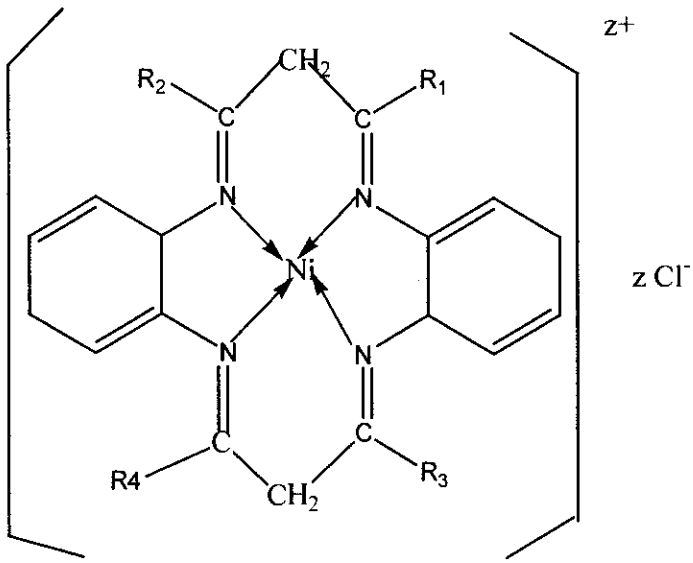

1- R_1=R_2=R_3=R_4=CH_3
2- R_1=R_3=CH_3, R_2=R_4=Ph

The electronic spectra of the other two Ni^{2+} complexes show two bonds within the ranges 15198-22963 cm^{-1} and 21032-24752 cm^{-1} assignable to the $^3A_{2g} \rightarrow {}^3T_{1g}(F)$ and $^3A_{2g} \rightarrow {}^3T_{1g}(P)$ transitions respectively in octahedral field. The values of magnetic moments 1.11-1.65 B.M. for these complexes are taken as additional evidence for an octahedral structure. The ligand field parameters (10 Dq and Racah parameter B) for these two complexes are calculated by solving equations 5 and 6, the values are given in Table (5), which are in the same range as reported for octahedral fields around Ni^{2+} ions[75,76].

$$\upsilon_1 ({}^3A_{2g} \rightarrow {}^3T_{2g}) = 10\,Dq \qquad (4)$$

$$\upsilon_2 ({}^3A_{2g} \rightarrow {}^3T_{1g}(F)) = 10\,Dq + \frac{15}{2}B - \frac{1}{2}[(15B - 6\,Dq)^2 + 64(Dq)^2]^{\frac{1}{2}} \qquad (5)$$

$$\upsilon_3 ({}^3A_{2g} \rightarrow {}^3T_{2g}(P)) = 15\,Dq + \frac{15}{2}B + \frac{1}{2}[(15B - 6\,Dq)^2 + 64(Dq)^2]^{\frac{1}{2}} \qquad (6)$$

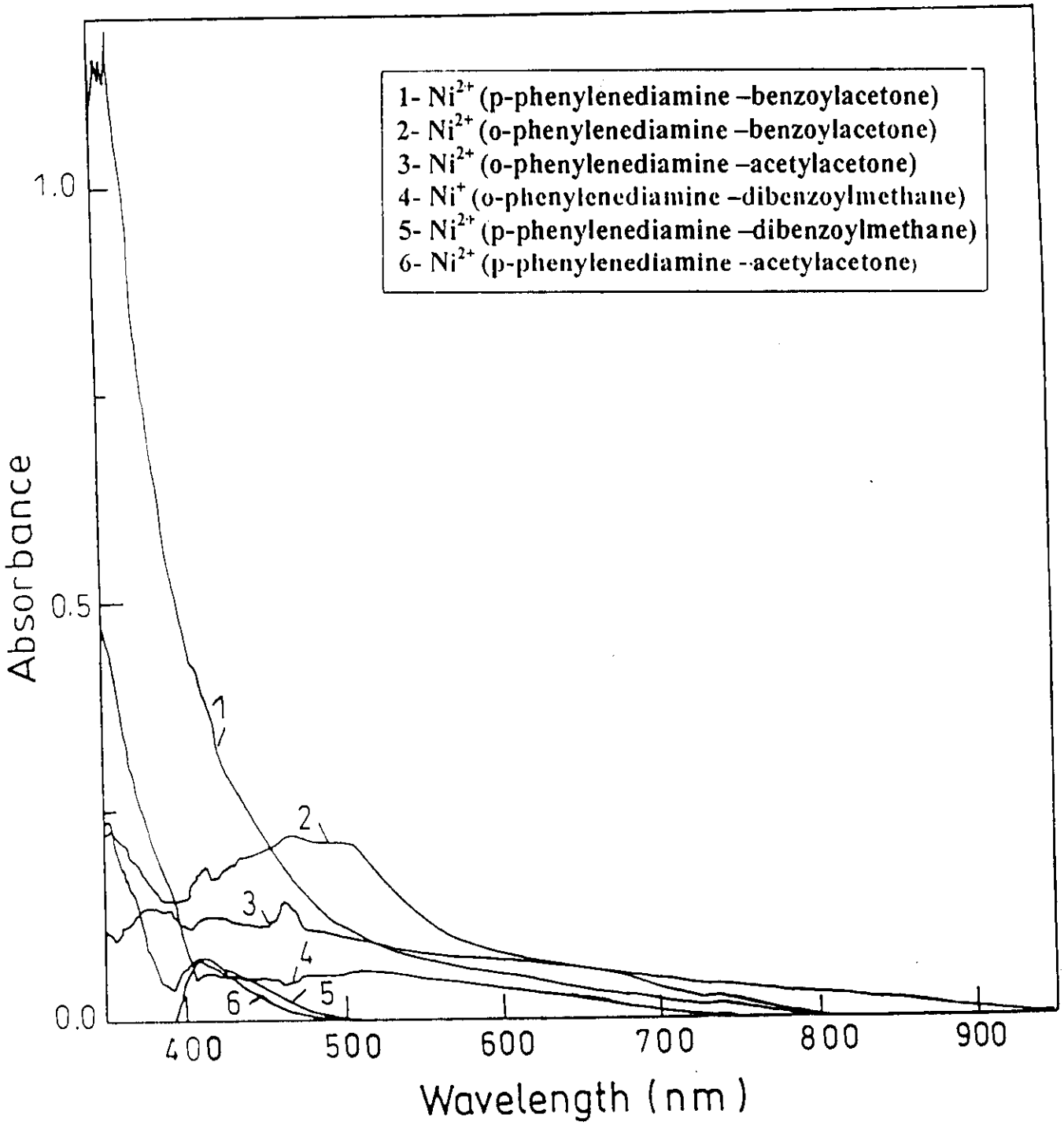

Fig. (18) Electronic absorption spectra of macrocyclic Ni^{2+} complexes in Nujul mull.

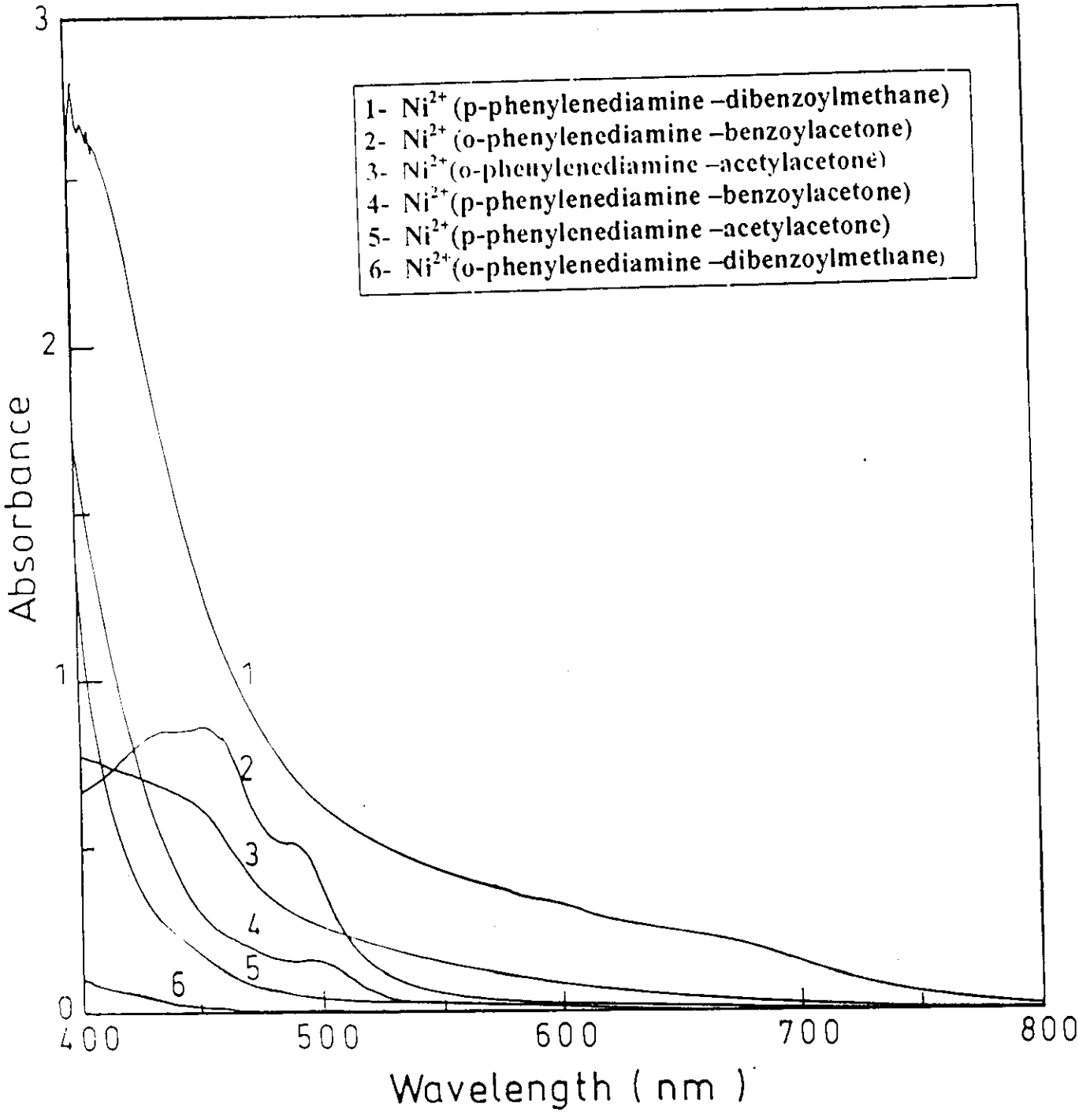

Fig. (19) : Electronic absorption spectra of macrocyclic Ni^{2+} complexes in DMF

5.4.4. Spectral and magnetic properties of Cu(II) macrocyclic complexes

The copper (II) ion ($3d^9$) has one unpaired electron in 3d-level. Its compounds are expected to show magnetic moments close to the spin only value, i.e. 1.73 B.M. based on theoretical calculation irrespective of the bond type involved. However, the observed values of the magnetic moments are 2.12 -2.38 B.M. for most copper(II) compounds with ionic or rather weak covalent bonds and 1.26-1.83 B.M. for compounds with strong covalent bonds. Also, copper (II) compounds having subnormal magnetic moments, less than 1.73 B.M. have recently been recorded. These subnormal moment values, measured at room temperature, were attributed to weak covalent bonds.

The d^9 configuration gives rise to the ^2D ground term. However, in an octahedral field the odd electron residues in an e_g orbital, and the ground term becomes ^2Eg rather than $^2T_{2g}$.

In octahedral copper (II) complexes, a single absorption band in the visible spectrum corresponding to ^2E_g -$^2T_{2g}$ is expected. In many copper(II) complexes, the Jahan-Teller distortion is so great that the coordination is almost of square planar type.

Orgel pointed out the validity of application of crystal field theory to explain the coordination in copper complexes according to the electron occupying the $d_{x^2-y^2}$ orbital. If any additional ligands are available they would take up the fifth and the sixth coordination positions. However, because the d_{z^2} always contains a lone pair of electrons, in most copper complexes the fifth and sixth ligands are in the plane and thus the complex

will have tetragonal structure. The square-planar geometry energy level diagram of one or nine d electrons is similar to that give in Fig.(5-7).

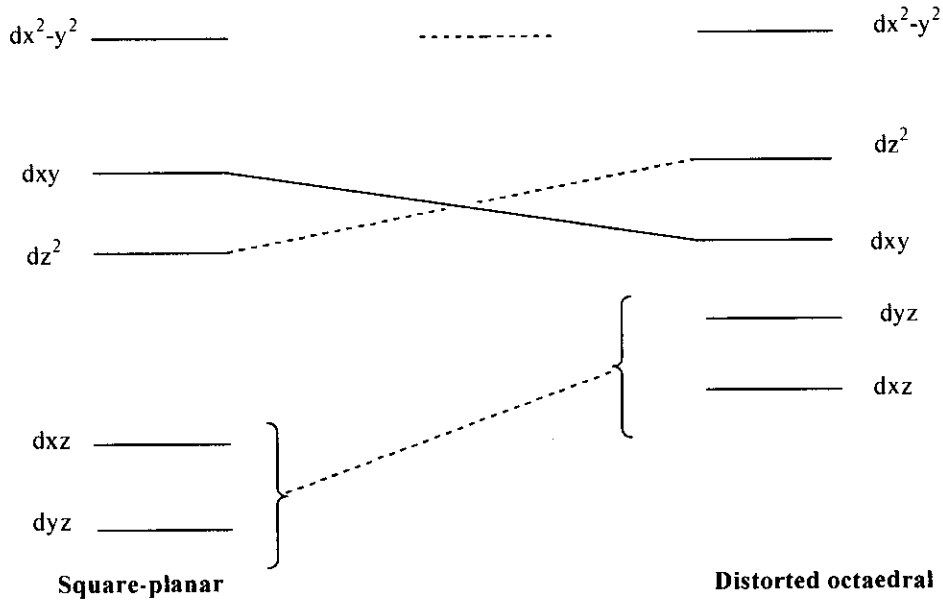

Fig.(5-7): Transition from square-planar to distorted octahedral

The isolated Cu(II) complexes have magnetic moment values (1.26-2.38 BM). No significant conclusion can be drawn from the magnetic data regarding the stereochemistry of the prepared copper(II) complexes. The electronic spectra of Cu(II) complexes show two broad band Figs. (20, 21) within 13774-20284 cm^{-1} and 16103-21459 cm^{-1} which can be assigned respectively to $^2E_{2g} \rightarrow {}^2B_{1g}$ and $^2A_{1g} \rightarrow {}^2B_{1g}$ transition in a tetragonally distorted octahedral configuration[75,76].

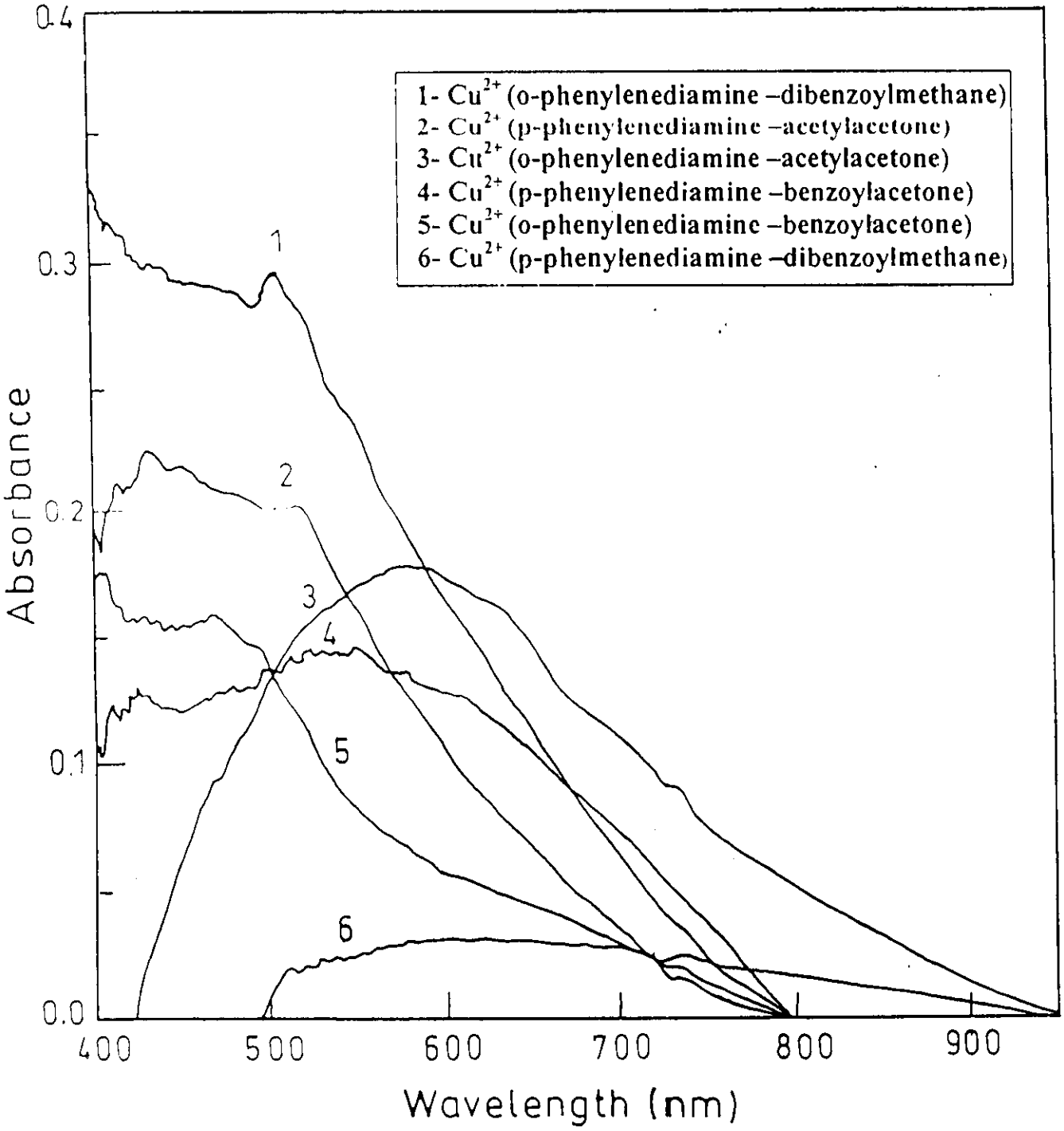

Fig. (20) : Electronic absorption spectra of macrocyclic Cu^{2+} complexes in Nujul mull.

6. Electron spin resonance spectroscopy of copper complexes:

Electron paramagnetic resonance (EPR) spectroscopy is a method to investigate the behavior of samples containing unpaired electrons (free radicals or compounds comprising an ion whose outer electronic shell is incomplete) in an applied magnetic field. It consists in recording the microwave energy absorbed by the sample as a function of the applied magnetic field. Two kinds of information may usually be obtained by this technique. The first one is a tensor characterizing the so-called Zeeman interaction, or interaction of the applied magnetic field with the unpaired electron(s). The second consists of tensors characterizing the interaction of the unpaired electron(s) with each type of nuclei possessing an intrinsic magnetic moment or spin, provided that this interaction is reflected by specific lines in the ESR spectrum.

The ESR spectra of transition metal complexes are affected mainly by spin-orbit coupling and ligand field strength. In order to obtain good information about ground and excited states in the complexes and the nature of bonding between the central metal ion and the ligand, the magnitude of "g" tensor must be calculated.

The Cu (II) ion with d^9 configuration has effective spin of $s = \frac{1}{2}$ and associated spin angular momentum, $m_s = \pm\frac{1}{2}$ giving rise to a doubly degenerate spin states in the absence of a magnetic field. In the presence of a magnetic field, the degeneracy is removed as Figure (22) and the energy difference between the two states is given by:

$$\Delta E = h\upsilon = g\,\beta\,H \qquad (6\text{-}1)$$

Where:

υ	is the frequency of microwave radiation	
H	is the strength of applied magnetic field	
β	is the Boher magneton,	and
G	is the land splitting factor	

In general, the deviation of g-value from that of the free spin "g_o" (2.0023) is mainly due to the perturbation of the ligand field, where:

$$g = g_0 - \frac{n\lambda}{\Delta} \qquad (6\text{-}2)$$

where:

n	is small integer
λ	is the spin-orbit coupling constant for the free ion ($\lambda = -829\ cm^{-1}$ for the gaseous Cu^{2+}).
Δ	is the energy separation between the ground and the excited states.

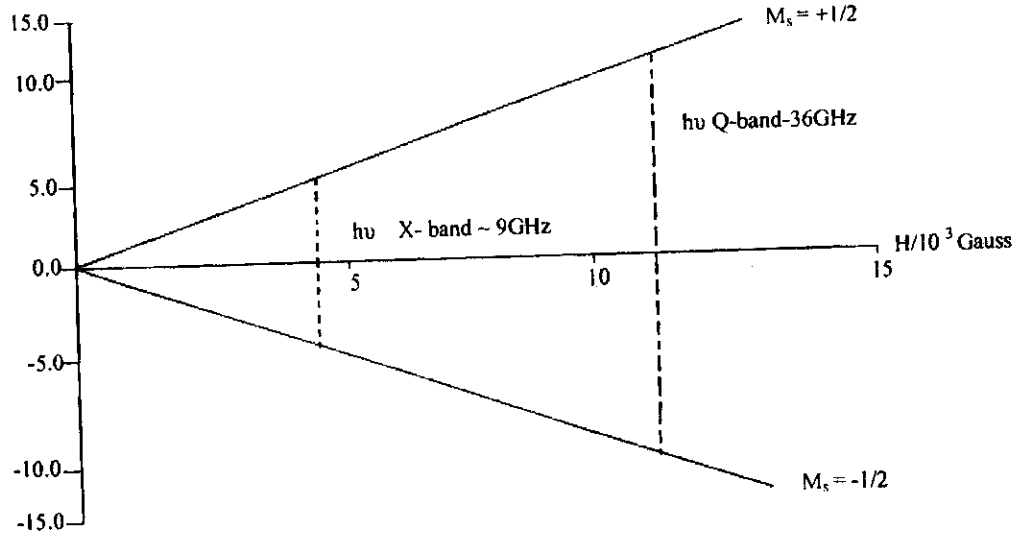

Fig.(22) : ***Effect of applied static magnetic filed (H) on an electron with "spin only" magnetism***

The g-factor is a dimensionless constant and its actual value for a free electron is 2.0023 but in transition metal complex, the unpaired electron is localized in a particular orbital. Thus, because of

(i) The loss of orbital degeneracy.

(ii) The spin-orbit coupling, the g-value for the complex is different from 2.0023. Its value depends on the relative magnitude of the spin-orbit coupling and the crystal field. The spin-orbit contribution makes "g" a characteristic property of a transition metal ion and its oxidation state.

From the g-value of transition complexes we can get very important information about their structure. In a cubic crystal field, the metal-ligand bond lengths are the same along all the three Cartesian axes, and hence $g_x = g_y = g_z$ and hence such a "g" is said to be isotropic. If the crystal field is tetragonal, the metal-ligand distances along the x- and y- axis are the same but different from the metal-ligand distance along the z- axis. Such a "g" is said to be anisotropic and is expressed as $g_x = g_y \neq g_z$. If the symmetry of a complex is rhombic, it should yield three different g values i.e. $g_x \neq g_y \neq g_z$.

The z-direction is defined coincident with the highest field rotation axis, then the g_z value is equivalent to $g_{\parallel}$ and the $g_{\perp}$ value obtained in any direction in the plane perpendicular to this direction

$$g_{\perp} = \frac{1}{2}(g_x + g_y) \qquad (6\text{-}3)$$

The g_{av} value for a tetragonal complex is given by:

$$g_{av} = \frac{1}{3}(g_x^2 + g_y^2 + g_z^2) = \frac{1}{3}(g_{\parallel}^2 + 2g_{\perp}^2)$$

or approximately as

$$g_{av} = \frac{1}{3}(g_{\parallel}^2 + 2g_{\perp}) \qquad (6\text{-}4)$$

- Tetragonally compressed Cu(II):

In this case the ground state is dz^2, and $g_\perp$ value is given by [78]

$$g_\perp = 2.0023 - \frac{6\lambda}{E_{dz2} - E_{dxy,\ dxz}} \qquad (6\text{-}5)$$

since λ is negative; $g_\perp > 2$ and also $g_\perp > g_\parallel$ where $g_\parallel = 2.0023$.

- Tetragonally elongated Cu(II):

In this case the ground state is $dx^2\text{-}y^2$, and the values of $g_\perp$ and $g_\parallel$ are given by

$$g_\perp = 2.0023 - \frac{2\lambda}{E_{dx2\text{-}y2} - E_{dxz,\ dyz}} \qquad (6\text{-}6)$$

$$g_\parallel = 2.0023 - \frac{8\lambda}{E_{dx2\text{-}y2} - E_{dxy}} \qquad (6\text{-}7)$$

Thus in this case $g_\parallel > g_\perp > 2.0023$.

-Square planar Cu(II):

In this case the unpaired electron resides in the $dx^2\text{–}y^2$ orbital and $g_\perp$ and $g_\parallel$ are given by

$$g_\parallel = 2.0023 - \frac{8\lambda}{E_{dx2\text{-}y2} - E_{dxy}} \qquad (6\text{-}8)$$

$$g_\perp = 2.0023 - \frac{2\lambda}{E_{dx2\text{-}y2} - E_{dxz,\ dyz}} \qquad (6\text{-}9)$$

so, we have $g_\parallel > g_\perp > 2$.

When the unpaired electron is in the dz^2 orbital, the g values are given by

$$g_\perp = 2.0023 - \frac{6\lambda}{E_{dz2} - E_{dxz,\ dyz}} \qquad (6\text{-}10)$$

$g_\parallel = g_e = 2.0023$

Thus $g_\perp > g_\parallel = 2$

The shifting of a g-value from 2.0023 in transition metal complexes is due to the mixing via spin-orbit coupling of the metal orbitals involved in molecular orbitals containing the unpaired electron(s), with the empty or filled ligand orbitals. When the mixing with the empty ligand orbitals, the result is negative "g" shift (g $+\Delta g$) is obtained when mixing with filled ligand orbital. The Δg value decreases as the covalency increases. For Cu(II) complexes, the $g_{\parallel}$ value is a sensitive parameter to indicate degree of covalency. For a covalent complex, $g_{\parallel} = 2.3$ or more.

For square planar Cu(II) complex, the g values are expressed as

$$g_{\perp} = 2.0023 - \frac{2K_{\perp}^{2}\lambda}{\Delta E_{yz}} \qquad (6\text{-}11)$$

$$g_{\parallel} = 2.0023 - \frac{8K_{\parallel}^{2}\lambda}{\Delta E_{xy}} \qquad (6\text{-}12)$$

where K's are the orbital reduction factor, ΔE_{xz} is the energy of the $^{2}B_{1g} \longrightarrow {}^{2}E_{g}$ transitions and ΔE_{xy} is the energy of the $^{2}B_{1g} \longrightarrow {}^{2}B_{2g}$ transition. From equations (6-11) and (6-12) we can get

$$G = \frac{4K_{\parallel}^{2}\,\Delta E_{xz}}{K_{\perp}^{2}\Delta E_{xy}} = \frac{g_{\parallel} - 2.0023}{g_{\perp} - 2.0023} \qquad (6\text{-}13)$$

Where G is the exchange interaction whose numerical value can be used as criterion for estimating where or not exchange coupling effects takes place between copper centers in the polycrystalline solid. If G> 4.0, considerable interaction in the solid complexes occurs and the ligand forming the complex is regarded as strong field ligand.

Different types of ESR spectra of copper(II) complexes are known[79,80]. They are (a); axial-elongated, (b); axial compressed, (c); rhombic-elongated, (d); rhombic-compressed, (e); isotropic and finally (f); compressed axial or rhombic symmetry with slight misalignment of axes (Fig.23).

The room temperature of ESR spectra of macrocyclic Cu(II) complexes with o-phynelenediamine-acetylacetone , p-phynelenediamine-acetylacetone and p-phynelenediamine - dibenzoylmethane (Figs 24-26), showed anisotropic spectra with $g_{\|} > g_{\perp}$ characteristic for distorted elongated tetragonal copper(II) complexes with $dx^2 - y^2$ ground state[79,80]. The analysis of the spectra gave the $g_{\|}$ and $g_{\perp}$ values as cited in Table (6). The g_{av} values were calculated from the relation:

$$g_{av} = \frac{1}{3} g_{\|} + \frac{2}{3} g_{\perp}$$

and given in Table (6).

The lowest g-value was found to be more than 2.0023, so tetragonal distorted symmetry associated with dx^2-y^2 state rather than dz^2 state is suggested[80].

The G values calculated using equation (6-13) amount to 4.79, 2.33 and 9.07 for Cu (o-phynelenediamine-acetylacetone), (p-phynelene-diamine-acetylacetone and (p-phynelenediamine-dibenzoylmethane) complexes respectively which indicate that interaction in the solid complexes takes place. The values of ΔE (cm^{-1}) corresponding to the $E_{dx2-y2} - E_{dxy}$ and $E_{dx2-y2} - E_{dxz,dyz}$ corresponding to the $^2B_{1g} \rightarrow {}^2E_g$ and $^2B_{1g} \rightarrow {}^2B_{2g}$ transitions respectively are also given in Table (7).

The polycrystalline X-band ESR spectrum of Cu(II) macrocyclic complex with o-phynelendiamine and dibenzoylmethane, Fig. (27), shows anisotropic nature characteristic of tetragonal compressed with dz^2 ground state and $g_{\perp}$ value > $g_{\|}$. The value of transition energy ($E_{dz^2} - E_{dxy,dxz}$) corresponding to $B_{1g} \rightarrow {}^2E_g$ was calculated and given in Table (7). Deviation in the g value of this complex from 2.0023 of free electron is

due to the covalence property as gathered from the G value (*C.f.* Tables 6,7)

The ESR spectra of Cu(II) complexes with benzoylacetone, o-phynelenediamine and p-phynlenediamine are shown in Figs. (28, 29). The spectra are splited giving rise to three g value. The weak and broad signals are due to the polymeric nature of these complexes. The broad signal is common in many copper complexes and is attributed to the dipolar broadening enhanced spin-lattice relaxation property. The g_{av} values are calculated from the relation

$$g_{av} = \frac{1}{3} (g_1 + g_2 + g_3)$$

and the R value is calculated by

$$R = \frac{g_2 - g_1}{g_3 - g_2}$$

The values of R are 2.11 and 2.01 for complexes Cu(o-phenylenediamine-acetylacetone) and Cu(p-phenylenediamine-benzoylacetone) respectively. i.e. R> 1 indicating dz^2 in ground state.

Table (6): ESR-Spectral Parameters of Copper (II) Complexes

No.	Complex	g_1 $g_{\|}$	g_2	g_3 $g_{\perp}$	g_{av}
19	Cu(o-phen-acac)	1.655	-	1.931	1.839
20	Cu(o-phen-Beac)	1.962	1.678	2.588	2.076
21	Cu(o-phen-dbmeth)	1.801	-	2.134	2.023
22	Cu(p-phen-acac)	1.530	-	1.801	1.711
23	Cu(p-phen-Beac)	1.725	1.931	2.134	1.930
24	Cu(p-phen-dbmeth)	1.666	-	2.044	1.918

Table (7): The values of ΔE (cm^{-1}) corresponding to $^2B_{1g} \longrightarrow {}^2E_g$ for Copper(II) Complexes

No.	Complex	$E_{dx^2-y^2} - E_{dxz,dyz}$ cm^{-1}	$E_{dx^2-y^2} - E_{dxy}$ cm^{-1}	$E_{dz^2} - E_{dxy,dxz}$ cm^{-1}	G	$K_{\|}$	$K_{\perp}$
19	Cu(o-phen-acac)	22932	19096	-	4.8	0.825	0.832
21	Cu(o-phen-dbmeth)	-	-	38951	1.58	0.63	1.13
22	Cu(p-phen-acac)	8195.7	14042	-	2.33	0.965	1.41
24	Cu(p-phen-dbmeth)	43979	19375	-	9.07	0.82	0.63

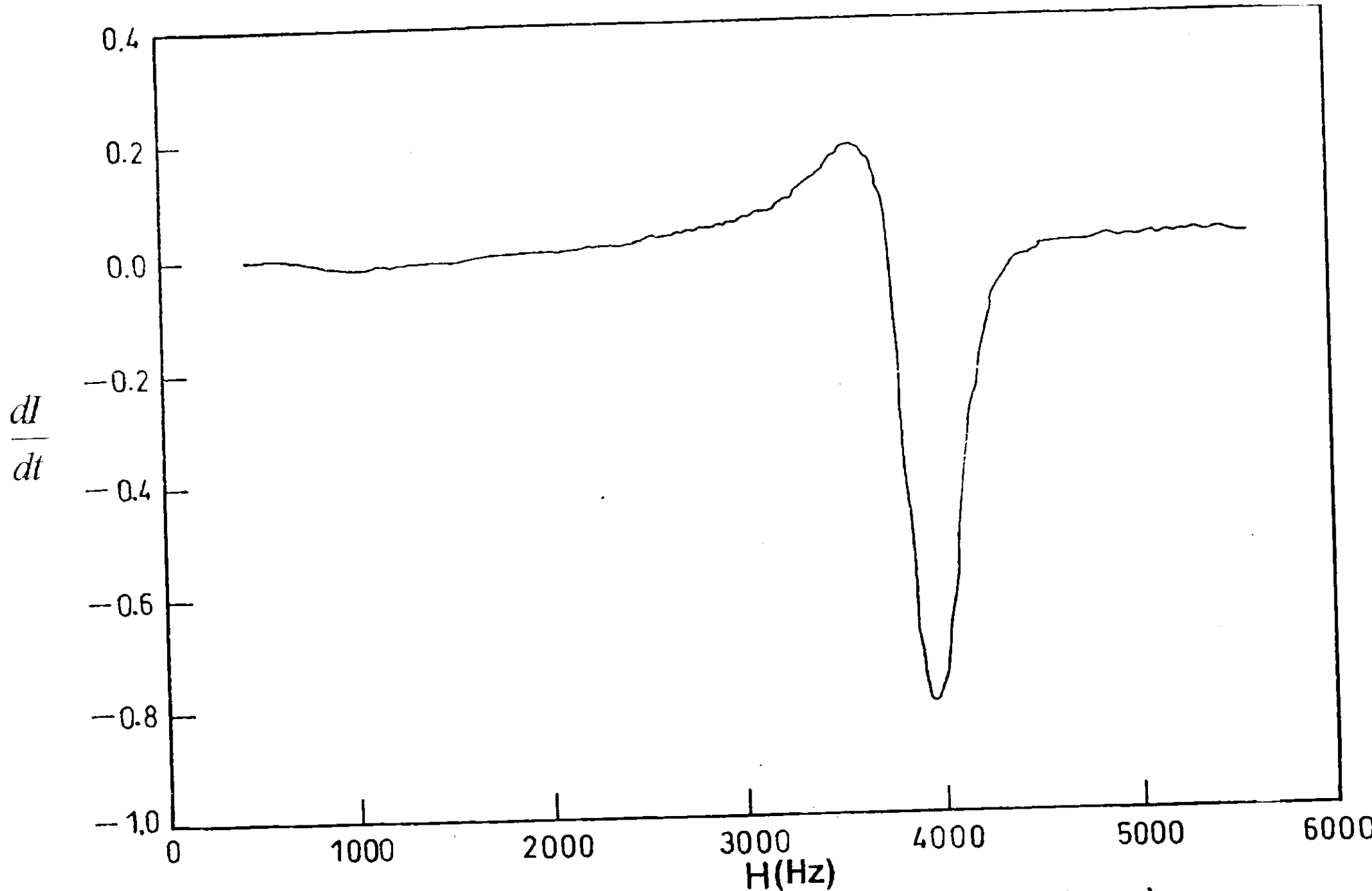

Fig. (24): ESR spectra of Cu^{2+} (o-phenylene diamine - acetyl acetone).

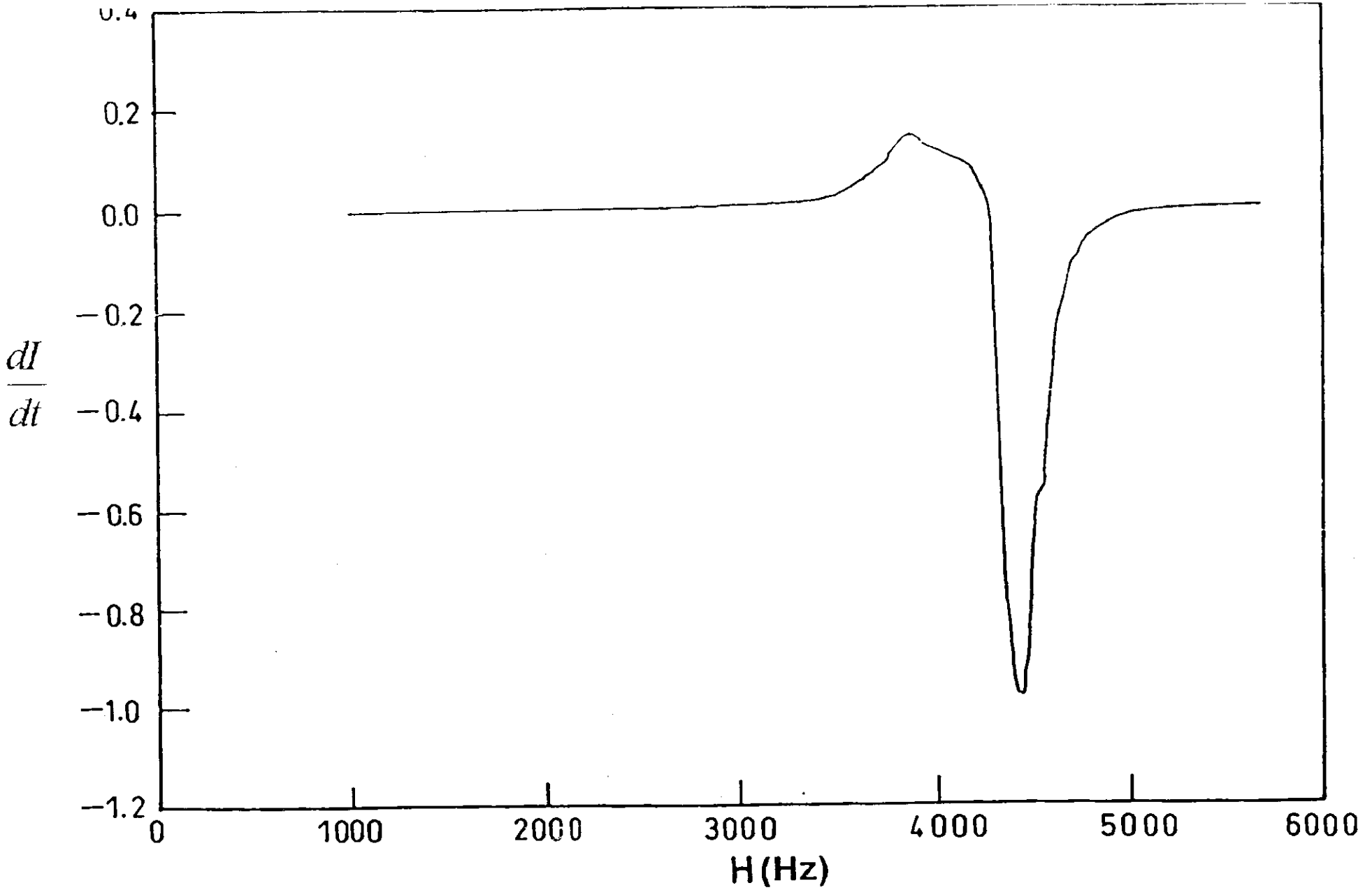

Fig.(25): ESR spectra of Cu^{2+}(p-phenylenediamine - acetyl acetate).

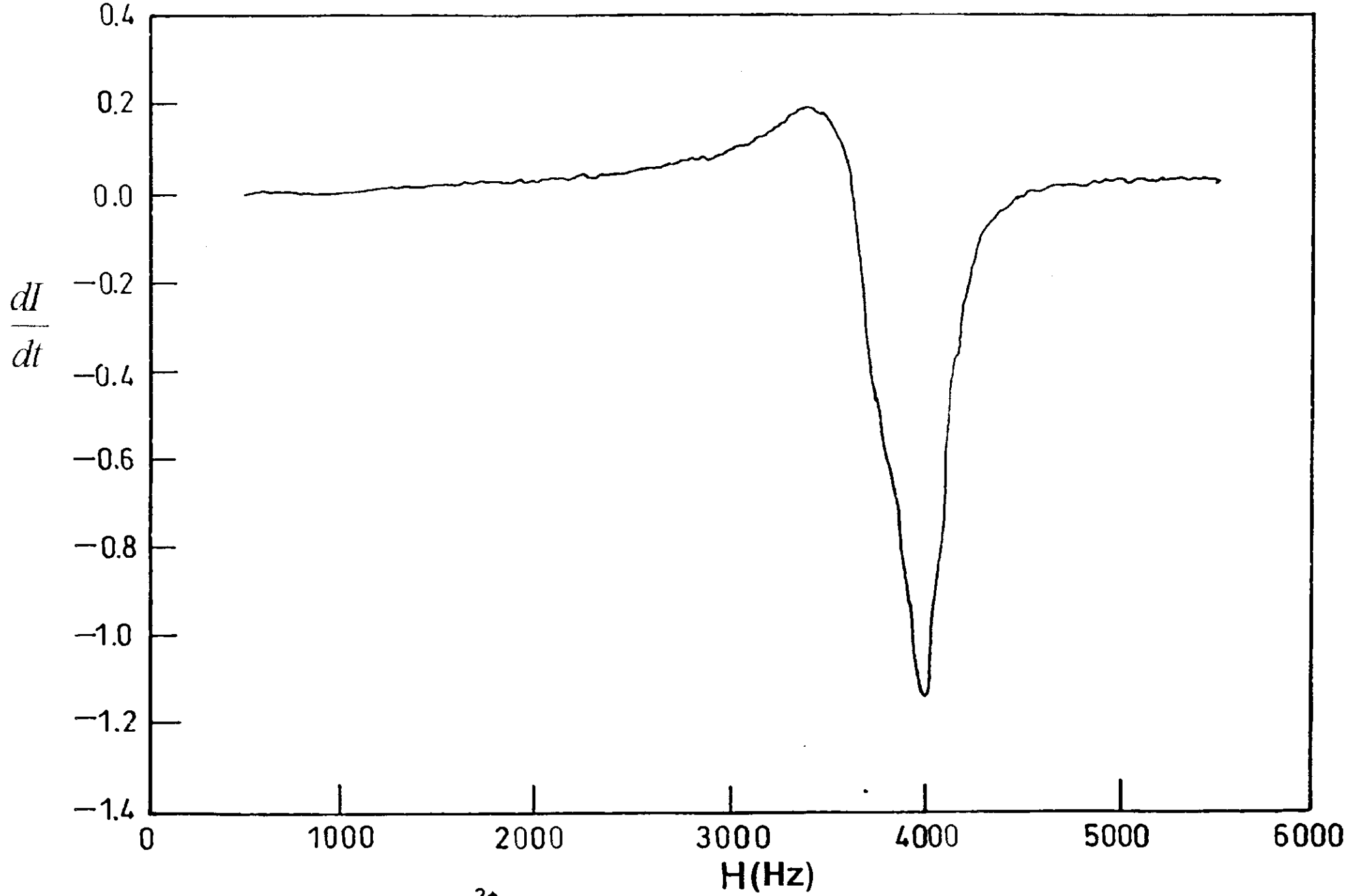

Fig. (26): ESR spectra of Cu^{2+} (p-phenylene diamine- Dibenzoylmethane).

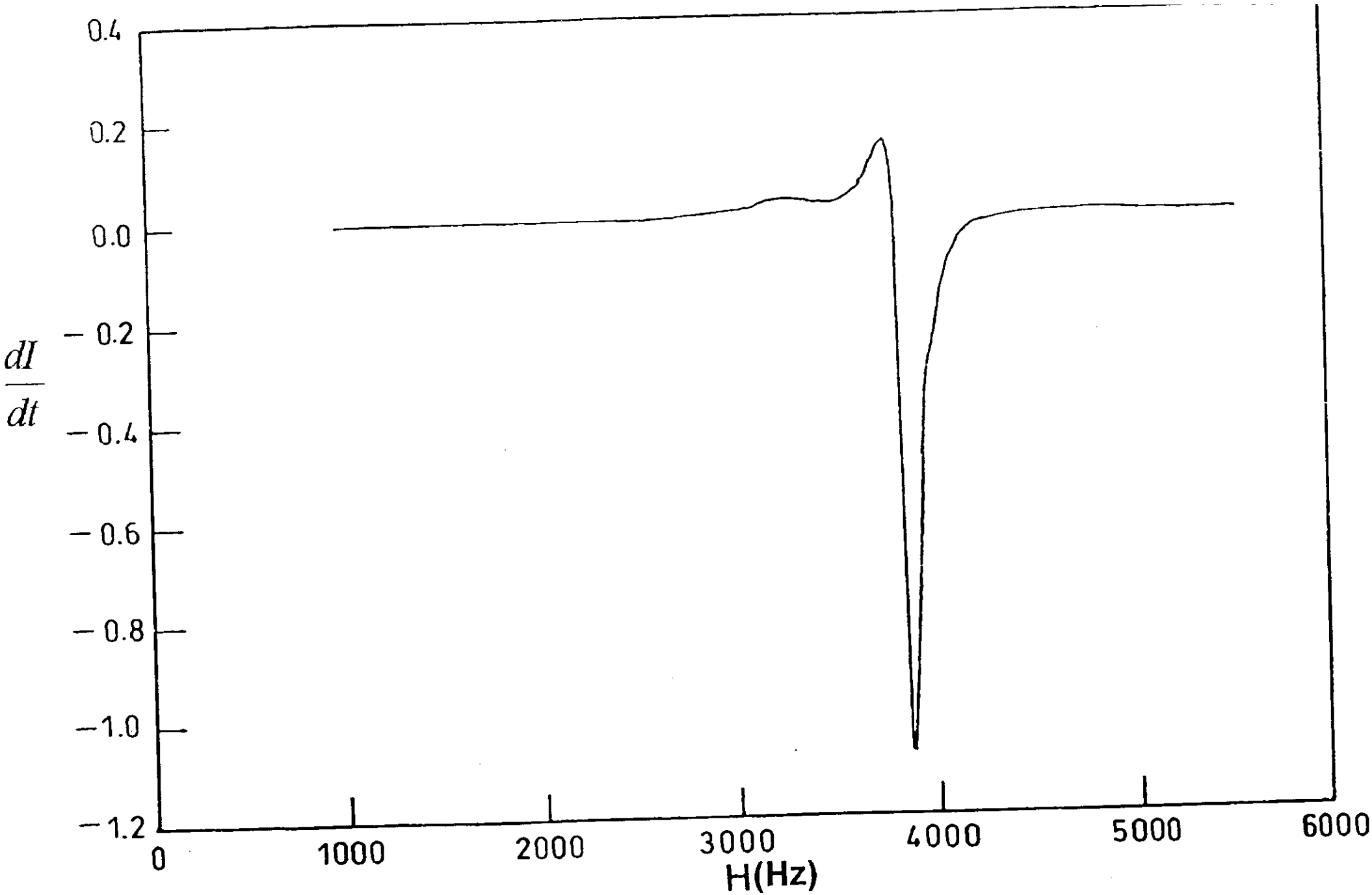

Fig. (27) : ESR spectra of Cu^{2+} (o-phenylenediamine - Dibenzoylmethane).

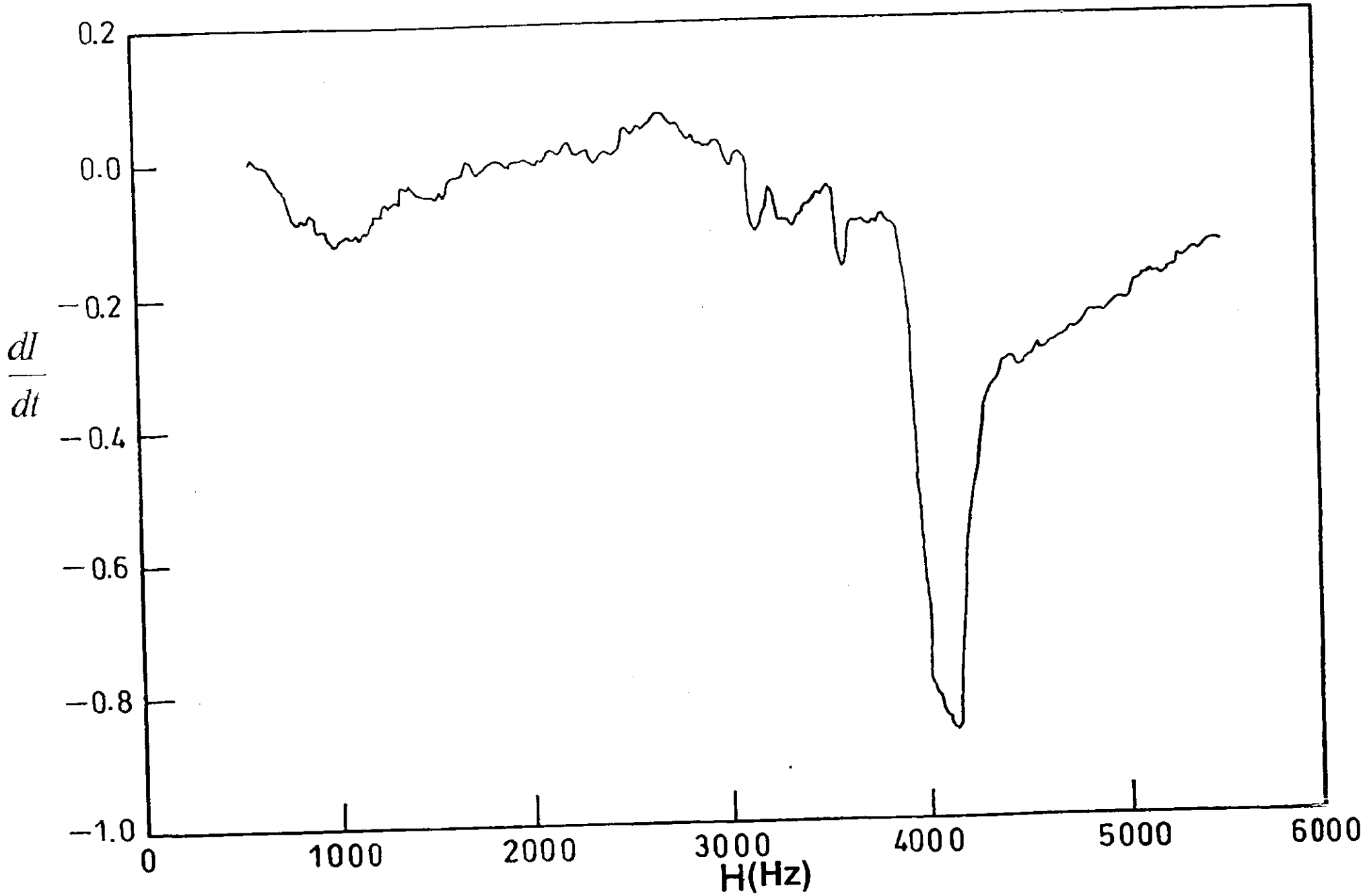

Fig.(28): ESR spectra of Cu^{2+}(o-phenylene diamine- Benzoyl acetone).

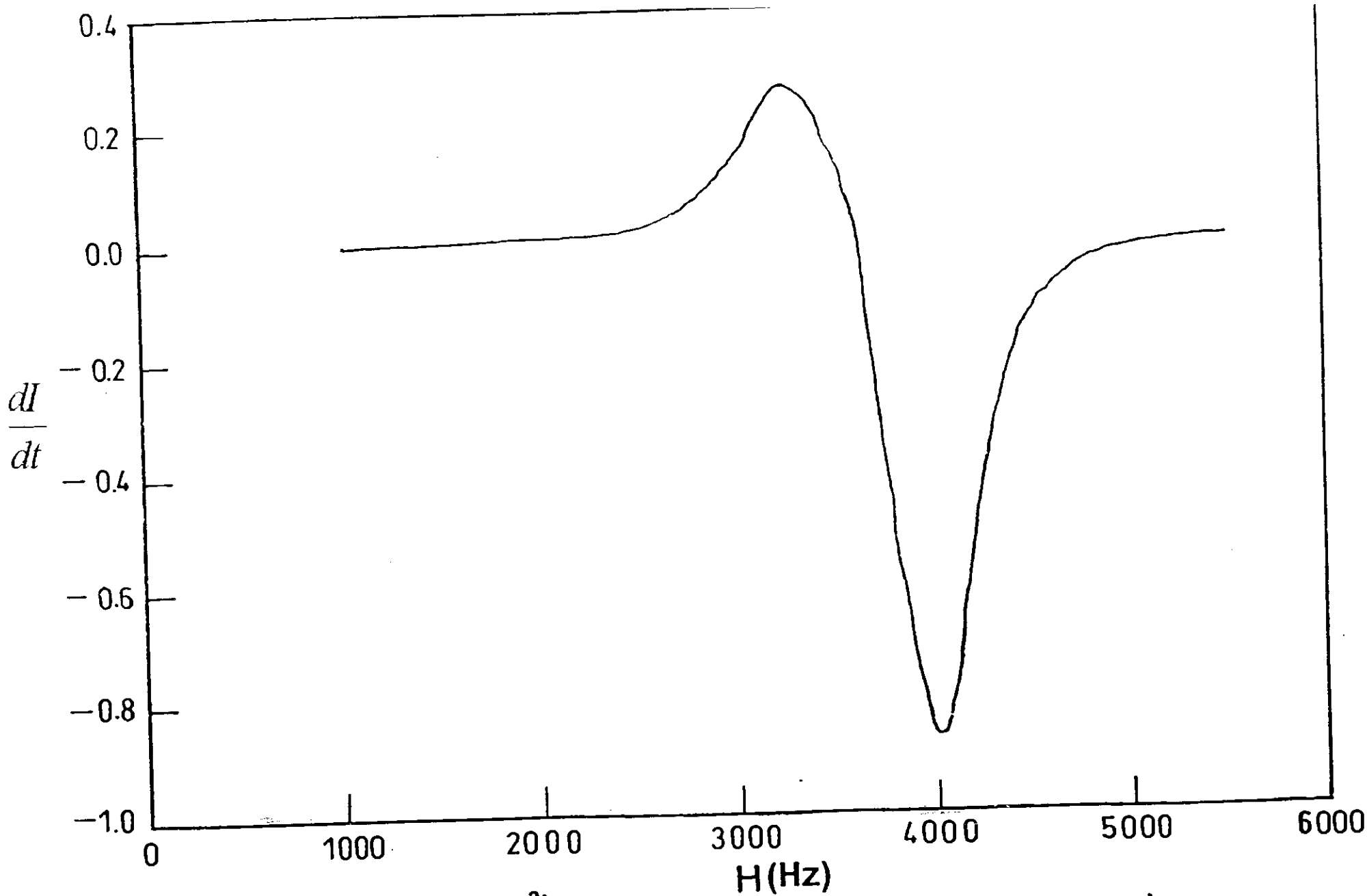

Fig.(29): ESR spectra of Cu^{2+} (p-phenylene diamine - Benzyl aceton).

7. X-Ray Diffraction Analysis

The X- Ray diffraction has been made for the Co^{2+}(o-phenylene-diamine-acetylacetone), Co^{2+}(o-phenylenediamine-benzoylacetone), Cu^{2+} - (o-phenylenediamine-acetylacetone) and Ni^{2+}(o-phenylenediamine-acetyl acetone) macrocomplexes. Figs. (30-33) show the XRD patterns of these macrocomplexes. All the prepared complexes show a peaks at 2θ about 5.5-15.7 Å that indicate the presence of layer structure. This can be illustrated in the light of the proposed structure of the macromolecules prepared. The XRD's also show the absence of a single phase structure.

8. Scanning Electron Microscope

Figure (34) Shows the SEM image of Cu^{2+} (o-phenylenediamine-acetyl acetone) macrocyclic complex. The micrograph shows a species of different size ranging from 50 μm up to 150 μm. The perfect shape of the particles give an indication that the prepared materials are composed of multiphase as represented from the XRD. It is also seem to have layer structure.

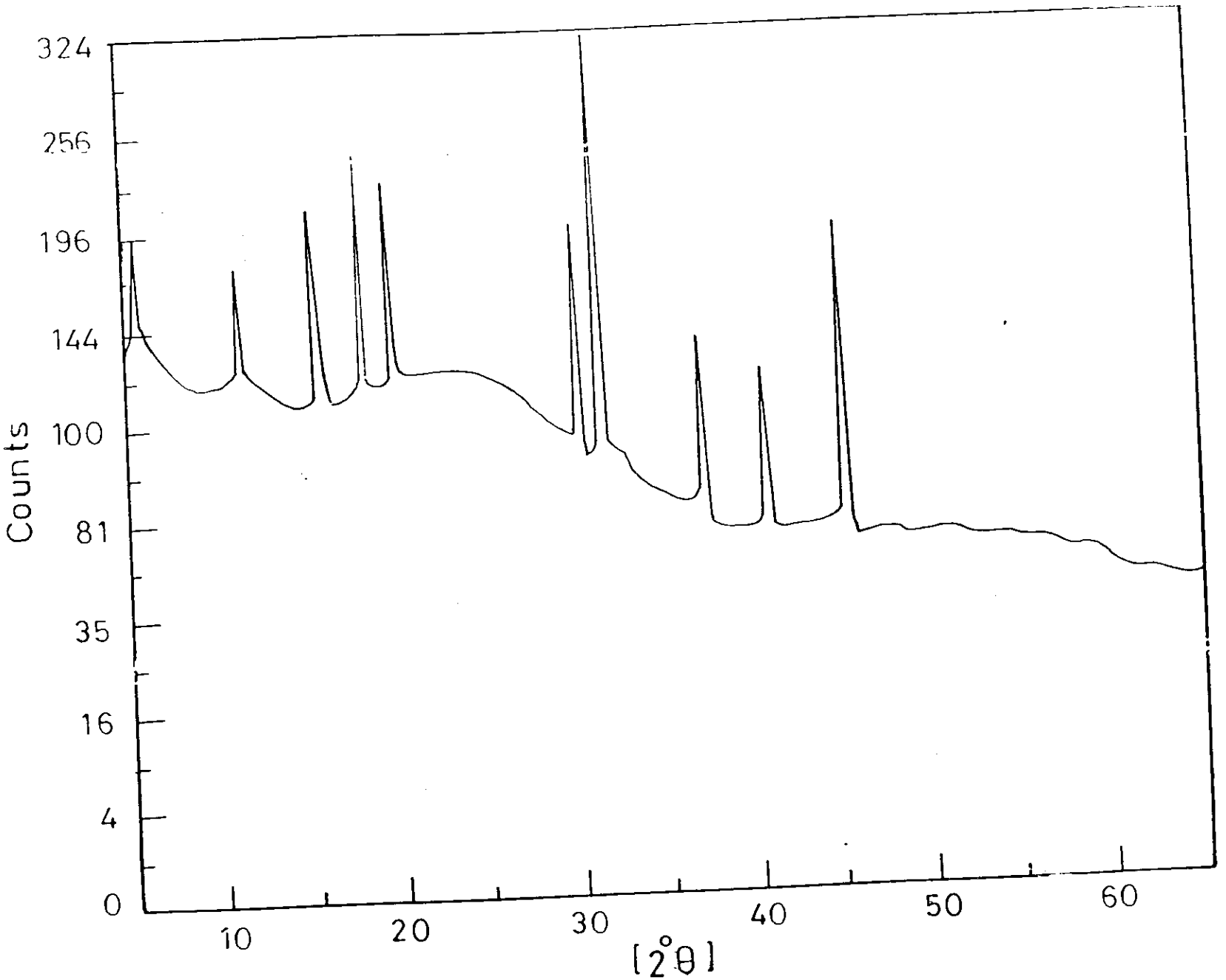

Fig. (30): The X-Ray diffraction of Co^{2+} (o-phenylene-acetylacetone.

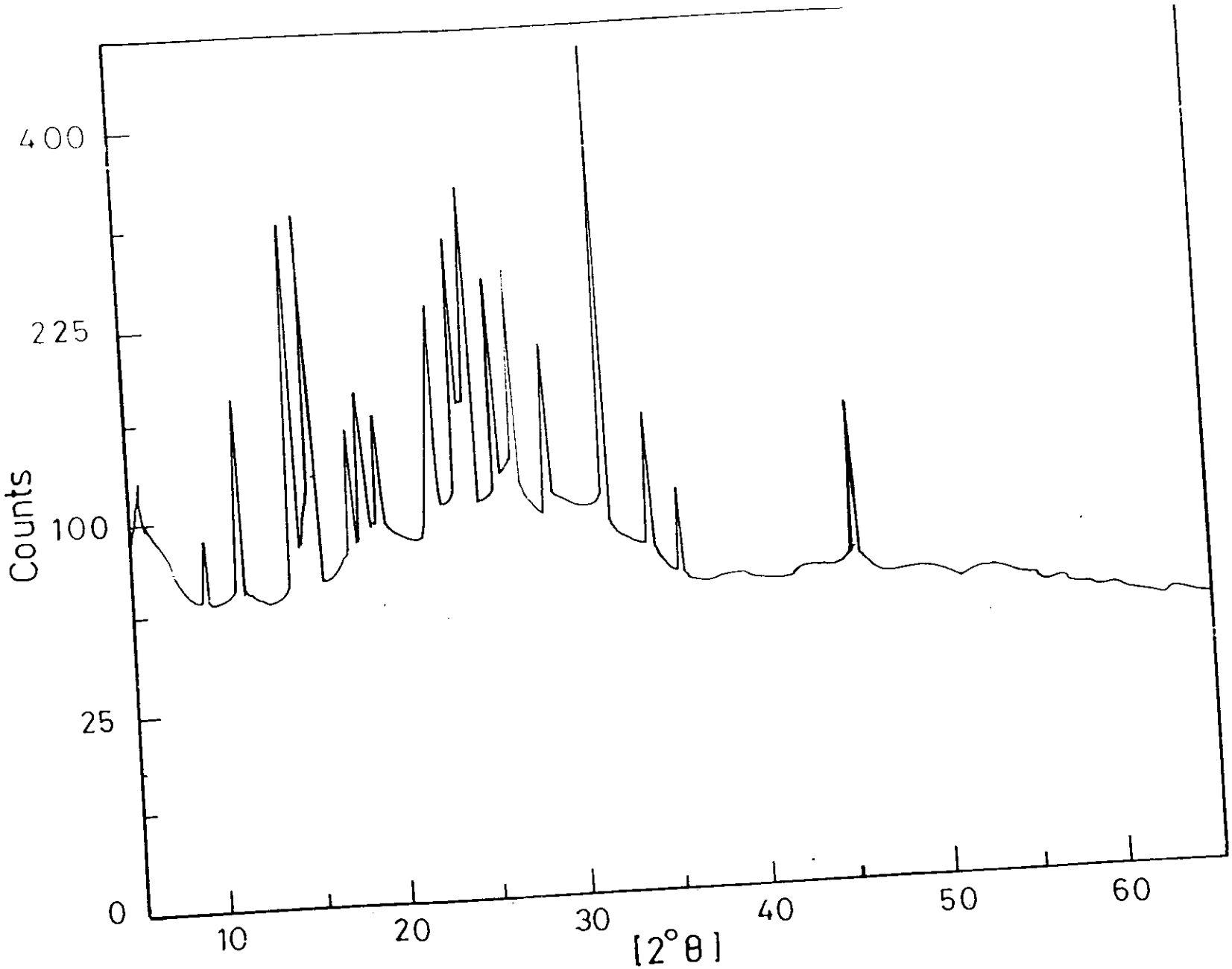

Fig. (31): The X-Ray diffraction of Co^{2+} (o-phenylene-Benzoylacetone).

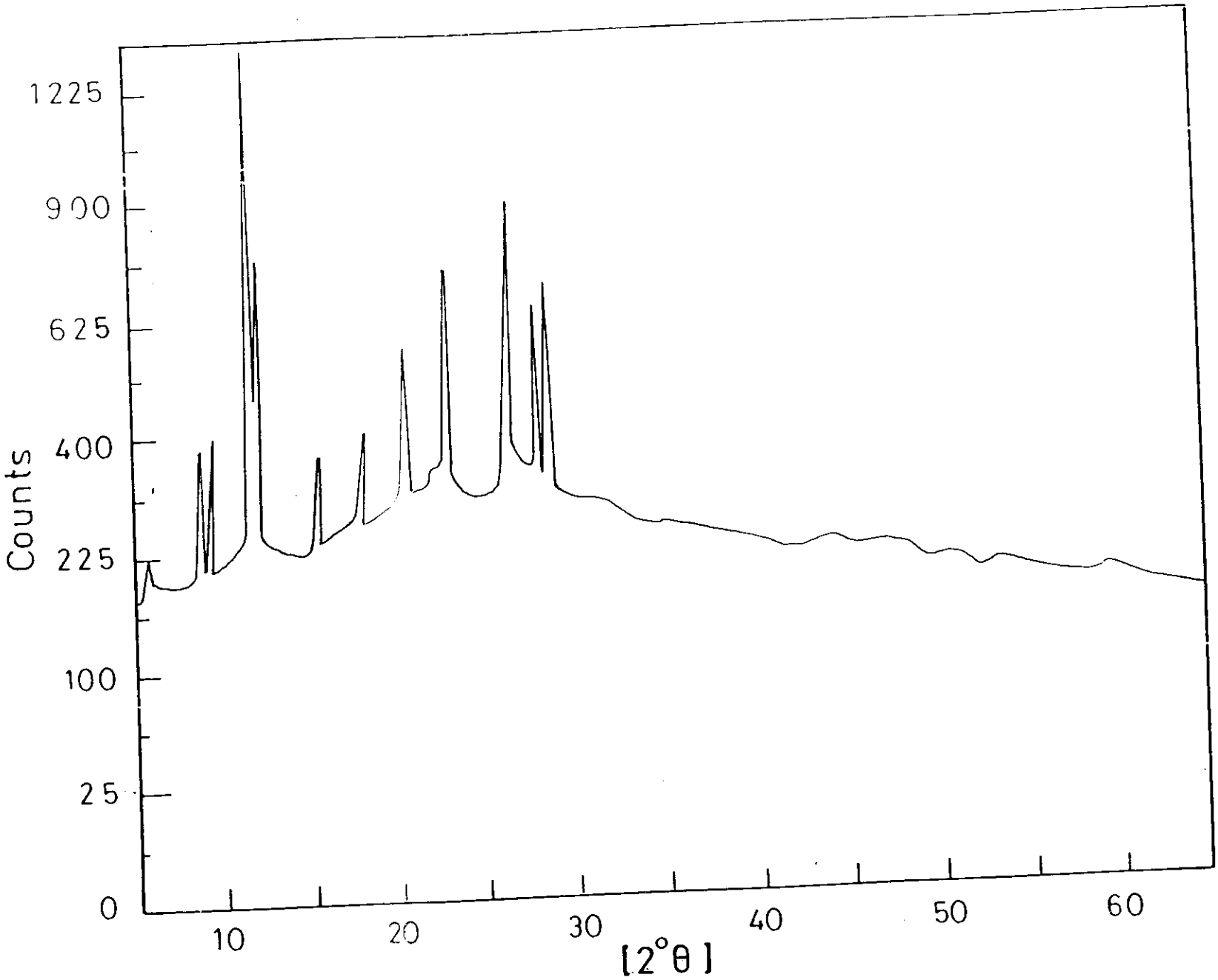

Fig. (32): The X-Ray diffraction of Cu^{2+} (o-phenylene-acetylacetone).

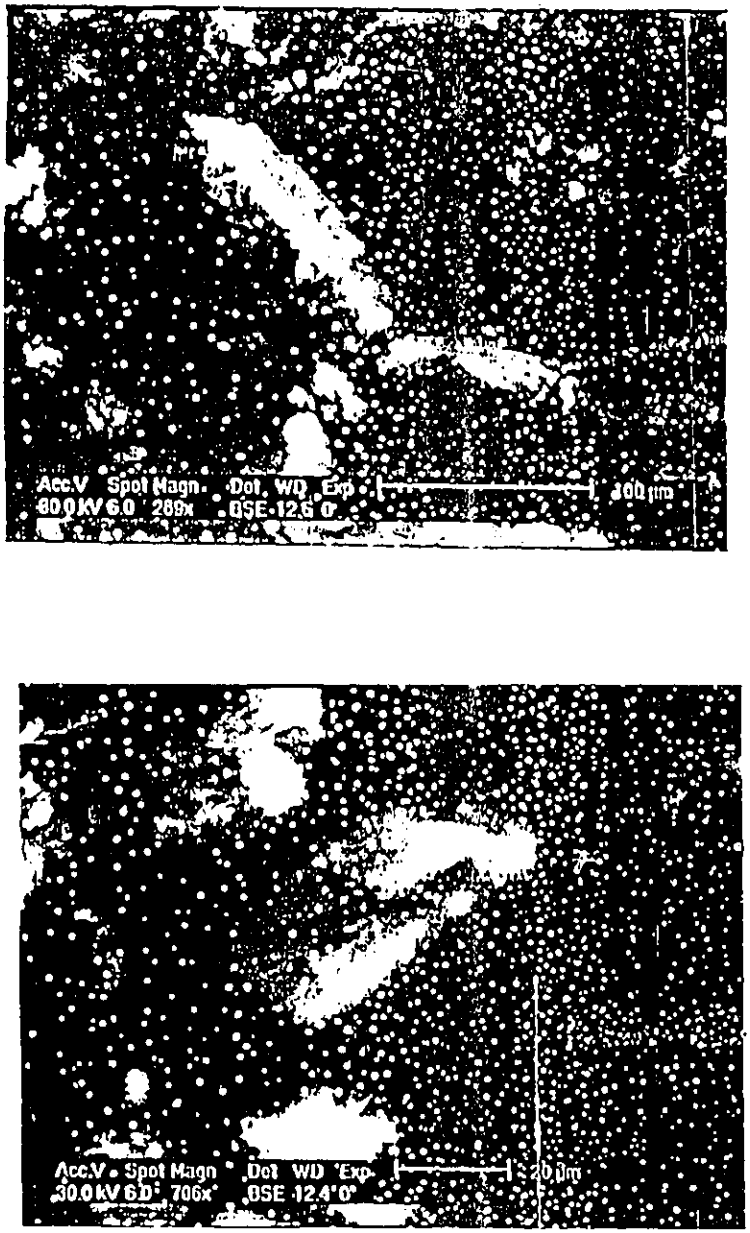

Fig. (34) : The SEM image of Cu^{2+}(o-phenylene-acetylacetone)